Biogeosciences Discuss., https://doi.org/10.5194/bg-2017-550
Manuscript under review for journal Biogeosciences
Discussion started: 19 January 2018

Biogeosciences Discussions Open Access EGU

Biogeochemical evidence of heterotrophic N_2 fixation in the Gulf of Aqaba (Israel), Red Sea

Angela M. Kuhn[1, 2], Katja Fennel[1], Ilana Berman-Frank[3]

[1]Department of Oceanography, Dalhousie University, Halifax, B3H 4R2, Canada
[2]Scripps Institution of Oceanography, University of California San Diego, La Jolla, 92093-0021, USA
[3]Mina and Everard Goodman Faculty of Life Sciences, Bar Ilan University, Ramat Gan, 5290002, Israel

Correspondence to: Angela M. Kuhn (angela.kuhn@dal.ca)

Abstract. Recent studies demonstrate that marine N_2 fixation can be carried out without light by heterotrophic N_2-fixers (diazotrophs). However, direct measurements of N_2 fixation in aphotic environments are relatively scarce. Heterotrophic, as well as unicellular and colonial photoautotrophic diazotrophs, are present in the oligotrophic Gulf of Aqaba (northern Red Sea). This study evaluates the relative importance of these different diazotrophs by combining biogeochemical models with time series measurements at a 700m-deep monitoring station in the Gulf of Aqaba. At this location, an excess of nitrate is present throughout most of the water column, especially in deep waters during stratified conditions. An excess of phosphate occurs only at the surface during nutrient-starved conditions in summer. We show that a model without N_2 fixation can replicate the observed surface chlorophyll, but fails to accurately simulate inorganic nutrient ratios throughout the water column. Models with N_2 fixation improve simulated deep nitrate by enriching sinking organic matter in nitrogen, suggesting that N_2 fixation is necessary to explain the observations. The observed vertical structure of nutrient ratios and oxygen is reproduced best with a model that includes heterotrophic, and colonial and unicellular autotrophic diazotrophs. These results suggest that heterotrophic N_2 fixation explains the observed excess nitrogen in deep water at this location. If heterotrophic diazotrophs are generally present in oligotrophic ocean regions, their consideration would increase current estimates of global N_2 fixation and may require explicit representation in large-scale models.

1 Introduction

Biological nitrogen fixation refers to the conversion of dinitrogen gas (N_2) via reduction to ammonium (NH_4) into bioavailable forms of nitrogen by a specialized group of microbes containing the nitrogenase enzyme complex. On geological timescales, the size of the oceanic reservoir of bioavailable nitrogen, and thus the ocean's capacity for exporting carbon, is controlled by the balance between removal of fixed nitrogen by denitrification and input by N_2 fixation (Falkowski, 1997; Haug et al., 1998; Deutsch et al., 2007; Gruber and Galloway, 2008; Fennel et al., 2005). The amount of organic matter exported from the surface to the deep ocean (i.e., export production) depends on allochthonous inputs of nitrogen (i.e., "new nitrogen") into the euphotic zone (Eppley and Peterson, 1979). These new nitrogen inputs determine the amount of "new production", which is directly related to the exported fraction. Locally the supply of new nitrogen can occur

Biogeosciences Discuss., https://doi.org/10.5194/bg-2017-550
Manuscript under review for journal Biogeosciences
Discussion started: 19 January 2018

through several mechanisms, including microbially mediated N_2 fixation, diapycnal mixing injecting deep nitrate (NO_3) into the surface, lateral transport and riverine input. While the injection of deep NO_3 is often regarded as the dominant source of new nitrogen and controlling the seasonal cycle of marine primary production; there is significant interest in better understanding the importance and quantifying the contribution of N_2 fixation to primary production, particularly in oligotrophic areas (Karl, 2002; Zehr and Ward, 2002; Capone et al., 2005; Luo et al., 2012).

Diazotrophs are able to produce nitrogenase, the catalyst enzyme for N_2 reduction, which is encoded by *nif* genes. *Trichodesmium spp.,* a group of non-heterocystous filamentous cyanobacteria that forms large colonies, was long considered the main contributor to N_2 fixation in the surface subtropical and tropical ocean (Carpenter and McCarthy, 1975; Capone et al., 2005). Increased sampling efforts and method improvements subsequently led to the discovery of a variety of other diazotroph groups including heterocystous endosymbiotic cyanobacteria (Zehr et al., 1998; Carpenter et al., 1999), free-living unicellular cyanobacteria (Zehr et al., 2001; Montoya, 2004; Moisander et al., 2010), and a number of cyanobacterial symbionts (Zehr et al., 2000). Most recently, genetic techniques have allowed the detection of *nif* genes in a number of anaerobic and heterotrophic phylotypes (Zehr et al., 2008; Zehr, 2011; Rahav et al., 2013, 2015). The abundance of *nif* genes does not necessarily imply that these organisms are actively fixing N_2 (Zehr et al., 2000; Moisander et al., 2017); however, the correlation between bacterial productivity and N_2 fixation rates suggests that significant aphotic N_2 fixation may occur in the Red Sea (Rahav et al., 2013, 2015). The differences in size and physiology of these diverse diazotrophs also suggest that they occupy distinct niches, and thus may affect primary productivity and export production differently (Bonnet et al., 2016; Moisander et al., 2010).

Most biogeochemical models treat N_2 fixation as a purely light-dependent, autotrophic process. These models either use mechanistic formulations of light limitation for the diazotrophic groups (e.g., Fennel et al., 2002; Moore, et al., 2004; Gregg, 2008; Dutkiewicz et al., 2012), or include theoretical considerations to introduce an empirical N_2 fixation flux in the model (e.g., Bisset et al., 1999). Some approaches neglect light limitation on diazotrophy and instead infer global N_2 fixation patterns from the distribution of dissolved inorganic nitrogen and phosphorus, and estimates of ocean circulation (e.g., Deutsch et al., 2007). In mechanistic models, diazotrophs are usually accounted for by a single functional group with biological rate parameters intended to represent either *Trichodesmium spp.*, unicellular cyanobacteria, or a generic autotrophic diazotroph. Only a few modelling studies have evaluated multiple autotrophic diazotrophs groups simultaneously, by considering separate groups for *Trichodesmium spp.*, unicellular cyanobacteria and diatoms-cyanobacterial associations (e.g., Monteiro et al., 2010; Dutkiewicz et al., 2012, 2015). To our knowledge, heterotrophic N_2 fixation has not yet been considered explicitly in biogeochemical models.

Understanding the ecological dynamics of different types of diazotrophs should significantly improve predictive capabilities in biogeochemical models, and lead to more accurate estimates of global N_2 fixation rates. It has been suggested that N_2 fixation rates are underestimated globally due to limited knowledge about the distribution and characteristics of N_2 fixing

organisms (Montoya, 2004; Zehr, 2011). It is also assumed that marine N_2 fixation may increase globally, as a result of ocean warming and higher concentrations of dissolved CO_2 in sea water (Hutchins et al., 2007; Levitan et al., 2007; Dutkiewicz et al., 2015).

In this study we explore the biogeochemical signatures that result from different assumptions about the ecological niches occupied by diazotrophs. We aim to answer the following two questions: i) How important is N_2 fixation as a source of new nitrogen in the Gulf of Aqaba? ii) How important is heterotrophic, light-independent N_2 fixation? To address these questions we implemented a one-dimensional model at a monitoring station for which monthly quality-controlled measurements of physical and biogeochemical variables are available from 2004 onward. We then systematically tested different model assumptions about diazotrophy and calibrated selected model parameters to facilitate an objective comparison between the different biogeochemical model versions. The different assumptions about diazotrophy consider the characteristics of organisms identified in the Gulf of Aqaba, including heterotrophic fixing α and γ proteobacteria (Rahav et al., 2013), unicellular cyanobacteria, and *Trichodesmium spp.* (Post et al., 2002; Foster et al., 2009; Rubin et al., 2012). Our most important conclusion is that aphotic N_2 fixation is necessary to reproduce the observed excess nitrogen in deep waters of the Gulf, while maintaining reasonable surface N_2 fixation rates. Our best performing biogeochemical model of the Gulf of Aqaba estimates annual N_2 fixation rates in overall agreement with local and large-scale estimates in the literature.

2 Study Area: The Gulf of Aqaba

The Gulf of Aqaba is a quasi-rectangular, 200-km long, 20-km wide, semi-enclosed basin in the northeast region of the Red Sea (Figure 1). The average depth of the Gulf of Aqaba is 800 m, its deepest point approximately 1800 m, and it is surrounded by arid mountains that steer the dominantly northerly winds (Berman et al., 2003). Two shallow sills, the Bab el Mandeb (~140 m) and the Strait of Tiran (~240 m), inhibit the entrance of cold and dense deep waters from the Indian Ocean. Since inflow is restricted to warm surface waters, the Gulf does not have permanent vertical stratification, the Gulf's deep water masses (>300 m) are locally formed (Wolf-Vecht et al., 1992; Biton et al., 2008) and have negligible horizontal transport toward the exterior (Klinker et al., 1976; Manasrah et al., 2006).

The annual hydrographic cycle exhibits a well-defined seasonality where vertical temperature and salinity distributions are dominantly affected by surface heat fluxes and modified by surface advective fluxes (Carlson et al., 2014). During winter (December to March), convective vertical mixing usually extends to depths >300 m (Labiosa et al., 2003), and even reaches the bottom (~700-800 m bottom depth) in some extreme years (Figure 2-3). From April to September, the water column is thermally stratified, and inflowing warm surface waters from outside the Gulf occupy the layer above the thermocline (Genin and Paldor, 1998; Berman et al., 2000; Biton and Gildor 2011). During fall (October to December), surface cooling and high evaporation rates erode the seasonal stratification and re-establish a well-mixed water column (Berman et al., 2003;

Monismith and Genin, 2004). The Gulf experiences net evaporation of approximately 1.6 m yr^{-1} (Ben-Sasson et al., 2009) due to negligible precipitation and run-off (Wolf-Vecht et al., 1992).

The Gulf is oligotrophic, with surface nitrate (NO_3) and phosphate (PO_4) concentrations usually close to their detection limits during summer stratification (Fuller et al., 2005; Mackey et al., 2009; Meeder et al., 2012). Deep winter mixing supplies inorganic nutrients to the surface, and NO_3 and PO_4 reach ~0.1 µM and ~2 µM, respectively (Figure 2; Lindell and Post 1995; Lazar et al. 2008). Dust from the desert provides a sufficient atmospheric source of soluble iron (Fe) for microbial growth in the Gulf (Chase et al., 2006; Chen et al., 2007). Phytoplankton spring blooms reach a maximum chlorophyll concentration of ~2 mg Chl-a m^{-3} and their initiation is strongly correlated with the termination of winter cooling of the water column (Zarubin et al., 2017). Interannual variability in the depth of winter convective mixing results in periods of nutrient accumulation in deep waters (Figure 2-3; Wolf-Vecht et al., 1992; Lazar et al., 2008; Carlson et al., 2012), which is re-set during extreme winter mixing events approximately every four years (Silverman and Gildor, 2008). The periodicity of these extreme mixing events has been associated with regional weather patterns that modify the Red Sea temperatures (Silverman and Gildor, 2008).

3 Methods

We analyzed the role of autotrophic and heterotrophic N_2-fixing organisms in determining biogeochemical patterns at an open pelagic site (Station A), located in the northern Gulf of Aqaba, by testing four alternative ecosystem model versions. The ecosystem models are evaluated in terms of their ability to replicate observations of oxygen (O_2), NO_3, PO_4, and chlorophyll. In this section, we first describe the available observations, then the models, and finally the systematic model calibration method.

3.1 Observations

Meteorological and oceanographic observations are available from the Inter-University Institute (IUI) for Marine Sciences in Eilat, Israel (http://www.iui-eilat.ac.il/Research/ NMPMeteoData.aspx). Meteorological observations are used to calculate surface heat and momentum fluxes for the physical model and incoming light for the biological models. Observed meteorological variables include wind speed, air temperature, air humidity, air pressure, irradiance and cloud cover. This data has been collected continuously and automatically at 10 min intervals by the meteorological instrumental array at the end of the IUI pier since 2006.

Monthly CTD and bio-chemical profiles at Station A (29.5° N, 34.9° E) were collected during monthly surveys of the National Monitoring Program (NMP) from 2004 to 2014 (http://www.iui-eilat.ac.il/Research/NMPMeteoData.aspx). CTD profiles are used to nudge temperature and salinity in the physical model (see section 3.2). Bio-chemical profiles, including NO_3, nitrite (NO_2), ammonium (NH_4), PO_4, O_2 and chlorophyll-a (Chl-a), are used for biogeochemical model calibration (years 2006 to 2010) and model validation against unassimilated data (years 2011 to 2014). Nutrients were measured using

spectrophotometry (QuickChem 8000 flow injection), O_2 was determined by Winkler titrations, and Chl-a concentrations are estimated using fluorometry (Turner Designs 10-AU).

3.2 Model Descriptions

The ecosystem models are implemented within the General Ocean Turbulence Model (GOTM), a one-dimensional physical model that computes solutions to differential equations for the vertical transport of momentum, salt and heat (Burchard et al., 1999). GOTM is implemented for the 700-m deep station with a vertical resolution of 3 m, and forced with hourly meteorological observations from the IUI pier. Temperature and salinity are nudged to observed CTD profiles with a nudging time scale of 30 days. This is done to account for the influence of horizontal advection of heat and salt in the one-dimensional model, and ensures a realistic representation of density stratification. The effect of temperature and salinity nudging on the results is analyzed below (section 4.2.1). As model calibration is computationally expensive, model simulations run only from January 2005 to September 2010. The first year of each simulation is considered model spin-up and excluded from further analysis (climatological meteorological forcing is used for the first year, as this database starts in 2006).

Four main ecosystem model versions of increasing complexity (referred to as H0, H1, H2 and H3) are treated as alternative hypotheses of how biological processes, especially diazotrophy, control the vertical distribution and temporal variability of dissolved inorganic nutrients and oxygen. H0 is the base model without explicit N_2 fixation (i.e., no diazotrophic plankton groups are included) and follows the model equations described in Fennel et al., (2006, 2013). We test this model with and without explicit inclusion of a sediment denitrification flux, denoted as H0 and H0', respectively. Thus, H0 fully neglects N_2 fixation, while H0' implicitly assumes that inputs from N_2 fixation and losses of fixed nitrogen due to denitrification are balanced.

H1, H2 and H3 are modified versions of H0, in which different groups of diazotrophic organisms are added sequentially. H1 introduces a generic autotrophic; H2 replaces H1's generic diazotroph with two autotrophs representing unicellular and colonial (e.g., *Trichodesmium spp.*) cyanobacteria. The unicellular group overall follows the same formulation as the generic diazotrophs, except that no aggregation term is included. We simplify unicellular diazotroph behaviour in this manner because this group represents free-living picoplanktonic cells that typically do not form large colonies although they can aggregate (Bonnet et al. 2016). Instead, we assume this group is grazed by zooplankton at similar rates as non-fixing phytoplankton. This difference between colonial and unicellular groups is consistent with studies suggesting that colonies represent an evolutionary adaptation to decrease grazing pressure (Nielsen, 2006). Aside from their size, *Trichodesmium spp.* colonies may be less palatable and harder to digest due to toxins (Kerbrat et al. 2010, 2011). Grazing is not a major fate of this group (O'Neil and Roman, 1994).

The last model version, H3, adds a heterotrophic diazotroph to the model structure of H2. This functional group is not limited by light, and grows by consuming both dissolved inorganic and organic phosphorus from detritus. In a subsequent set

Biogeosciences Discuss., https://doi.org/10.5194/bg-2017-550
Manuscript under review for journal Biogeosciences
Discussion started: 19 January 2018

of four experiments (H3a, H3b, H3c, and H3d), we remove complexity from H3. The heterotrophic group remains, but we sequentially remove the autotrophic groups one-at-a-time: first the colonial cyanobacteria (H3a), then the unicellular cyanobacteria (H3b), then the generic autotrophic diazotroph (H3c), and finally we remove all autotrophic diazotrophs (H3d). A summary of all model versions is given in Table 1 and a description of state variables and full model equations in the Supplement.

We acknowledge that some of these model assumptions are still simplifications of diazotroph behaviour. For example, *Trichodesmium spp.*, as well as other autotrophic and diazotrophic organisms, may also take up dissolved organic matter to support growth (Benavides et al., 2017). Nevertheless, model assumptions and formulations used here are in line with the most commonly accepted understanding of the dominant controls on microbial and diazotrophic growth.

3.3 Model Parameters

3.3.1 Parameter Optimization Method

Parameter optimization, i.e. the minimization of misfit between model and observations by adjusting model parameters, was applied to systematically calibrate the models. We used an evolutionary algorithm, where changes in the parameter values follow a set of rules inspired by the process of natural selection (Houck et al., 1995; Kuhn et al., 2015). The algorithm starts with a randomly generated "population" of 30 parameter sets $\{\vec{p}\}$, which are iteratively modified over a number of generations. During each generation of the population, the cost $J(\vec{p})$ of the model with parameter set $\vec{p}$ is calculated as:

$$J(\vec{p}) = \frac{1}{V}\sum_{v=1}^{V}\frac{w_v}{N}\sum_{i=1}^{N}\left(\hat{y}_{v,i} - y_{v,i}\right)^2, \quad (1)$$

where $\hat{y}$ represents a model estimate and y the corresponding observation. N is the number of observations included for each variable v. Here the number of variables V is 5 (nitrate + nitrite, ammonium, phosphate, chlorophyll-a, and oxygen measured as profiles at Station A between 2006 and 2010). Model-data misfits are weighted by the factor $w_v = 1/\sigma_v$, i.e, the inverse standard deviation of each variable. Half of the parameter sets with the lowest J value "survive" to the next generation. The other half of the population is regenerated from new parameter sets obtained by recombination of two random "parent" sets drawn from the better performing half (i.e., the "survivors" of the previous generation). Parameters also "mutate", i.e. random noise is added, for additional variability in the parameter space. An allowable range of values is set for each parameter based on the literature (Table 2).

3.3.1 Optimized Parameters

The parameter optimization method has limitations. Most importantly, the optimization cannot estimate with confidence parameters that are unconstrained by the observations (Fennel et al. 2001; Schartau and Oschlies, 2003; Ward et al., 2010). To avoid this, a subset of H0's most sensitive parameters was selected for optimization through a preliminary sensitivity analysis. Optimized parameters for H0 are identified in Table 2 along with the optimal values. The optimization was

replicated 10 times over 100 generations using the algorithm described in section 3.3.1. Non-optimized parameters are fixed at their a priori estimates based on Fennel et al. (2006, 2013).

For each model version with diazotrophs (H1, H2 and H3), some of the parameters already optimized for H0 required re-calibration to properly accommodate the changes in system dynamics. Re-calibrated parameters for each model version are presented in Table 3. No re-calibration was performed for model versions (H0' and H3a-d), as they are aimed to test the relative importance of individual model components.

3.3.2 Diazotroph Parameters

Since none of the parameters directly related to the diazotroph groups are constrained by the available observations, they were predefined for H1, H2 and H3, based on the observational and modelling literature (Table 3). Previous modelling studies have used maximum growth rates of generic N_2 fixers ranging from 0.4 d^{-1} (Moore, et al., 2004) to 1.25 d^{-1} (Ward et al., 2013). When model diazotrophs are assumed to represent *Trichodesmium spp*. values range between 0.17 d^{-1} (Hood et al., 2001) to 0.3 d^{-1} (Fennel et al., 2002). From the observational literature, *Cyanothece* (unicellular cyanobacteria) and *Trichodesmium spp.* cultured under various combinations of Fe and light availability exhibit maximum rates around 0.3 ± 0.05 d^{-1} (Capone et al., 1997; Berman-Frank et al., 2001; Hutchins et al., 2007). Growth rates can be higher (up to 0.43 d^{-1}) at high CO_2 and high light availability (Kranz et al., 2010). We chose a common reference maximum growth rate of 0.25 d^{-1} for all photosynthetic diazotrophs, such that differences between the model versions result only from the different assumptions about the losses of each group (e.g., predation of unicellular cyanobacteria vs. sinking of large aggregates). Based on growth rates measured for cultured heterotrophic bacteria, we chose a value of 0.2 d^{-1} for the heterotrophic diazotrophs (Pomeroy and Wiebe, 2001). Observational and modelling studies were also considered to set the photosynthetic initial slope of photosynthetic diazotrophs (Geider et al., 1997; Moore et al., 2004; Hutchins et al., 2007). Other parameters are based on Fennel et al. (2002).

4 Results

4.1 Observed NO_3 and PO_4 Patterns

To provide context for the evaluation of our model simulations, we first describe the observed interannual and seasonal variability of NO_3 and PO_4 for the complete time series (2004 to 2014) at Station A (Figure 2). From May to January vertical distributions of NO_3 and PO_4 show depletion of nutrients in the euphotic zone and a nutricline between 100 and 200 m. From February to April, nutrient concentrations increase near the surface and decrease in deep waters (>200 m) as result of vertical mixing. Multi-year periods of accumulation of nutrients in deep waters were observed from: i) the beginning of the series to the end of 2006, ii) after the winter of 2008 until February 2012, and iii) after the winter of 2013 until the end of the series. These periods are bookended by winters with extremely deep mixing events in 2007, 2008, 2012 and 2013 during

which nutrient concentrations are nearly homogenized in the entire water column. Two prolonged periods of these vertically homogenous conditions were observed in 2007 and 2008, lasting two to three months.

Our model calibration simulations are from 2006 to 2010, allowing us to include two years with deep winter mixing (2007 and 2008) and two years with moderate winter mixing (2009 and 2010). Figure 3 shows the linear metric N* (N*=DIN-16DIP) for our simulation period which quantifies excess and deficit of nitrogen relative to phosphorus with respect to the canonical Redfield ratio (N:P=16:1). This metric thus allows diagnosing patterns of net nitrogen addition, i.e. the balance of N_2 fixation and denitrification, on global and local scales (e.g., Gruber and Sarmiento, 1997). Using the Redfield ratio as a reference, N* is insensitive to changes in nutrient concentrations that result from nutrient uptake by non-fixing phytoplankton and remineralization of organic matter, assuming these processes occur in Redfield stoichiometry. Positive N* reflects an excess of nitrogen (DIN) and can be interpreted as a signature of N_2 fixation.

N* values presented in Figure 3 are calculated using the observations from Figure 2. Excess nitrogen (between +0.20 and +1.06 mmol N m^{-3}) dominates throughout most of the water column, except at the surface during stratified summer conditions, when nutrients are depleted and surface waters exhibit an excess of phosphate (-0.35± 0.25 mmol N m^{-3}). Waters with excess nitrate are brought to the surface during winter; however, N* values rapidly return to negative at the surface. The magnitude and duration of positive surface N* values appear to be related to the depth of winter mixing.

4.2 Model Results

4.2.1 Sensitivity to Physical Nudging

Model runs, with and without temperature and salinity nudging towards observations, demonstrate that nudging has a negligible effect below 200 m, indicating that horizontal advection does not modify the lower part of the water column in a significant way (Supplement). Above 200 m, nudging corrected model errors in the representation of vertical mixing and surface forcing. The average magnitude of the differences due to nudging in the top 200 m is 0.20±0.45 ºC and 0.5±0.16 kg m^{-3}. Since these effects are small and limited to the surface, we conclude that neither nudging nor the neglect of horizontal advection affects our conclusions.

4.2.2 Effects of N_2 Fixation on DIP and DIN

Figure 4 shows simulated NO_3 and PO_4 concentrations from models H0', H0, H1, H2 and H3, along with the corresponding measurements. Observed NO_3 and PO_4 concentrations exhibit a marked increase in deep water after the strong winter mixing of 2008. Weaker winter mixing after 2008 results in deep-nutrient accumulation, which is more pronounced for NO_3 than PO_4. Model H0' reproduces some deep-nitrate accumulation, but underestimates NO_3 concentrations in comparison to observations. Model H0 strongly underestimates inorganic nitrogen below the nutricline. Model H1, where N_2 fixation was introduced via a generic autotroph, generates only small changes in the vertical distribution of nutrients. In model H2 the

representation of NO_3 below the nutricline is slightly improved; however, underestimation of mid-water NO_3 and PO_4 is still noticeable. Model H3 significantly improves the representation of deep NO_3 accumulation.

These model differences are summarized in Figure 5, which shows the simulated and observed NO_3 and PO_4 inventories in surface and deep waters. According to the observations deep NO_3 accumulates between 2007 and 2010 at a rate of 0.59 ± 0.08 mmol m^{-2} d^{-1}, whereas deep PO_4 accumulates at 0.015 ± 0.009 mmol m^{-2} d^{-1}. During this accumulation period approximately 36 mmol NO_3 per mmol PO_4 appear in deep waters. All five model versions simulate similar magnitudes and temporal variability of PO_4, but NO_3, in particular below 100 m, diverges over time among the models. H0 has the largest deviations from the other models, simulating approximately constant deep NO_3 after 2007. H0', the version without denitrification, produces a rate of increase in deep NO_3 similar to that of model version H2. H3 has the highest accumulation rate of deep NO_3, matching the observed slope the best.

The PO_4 versus NO_3 plots in Figure 6 visualize these results in terms of N* values. Observed N* values above 200 m depth can become negative at low nitrate concentrations but are positive at intermediate nutrient concentrations. Below 200 m, observed N* values are positive. This observed pattern in the distribution of nutrients and N* values is not replicated by models H0 and H1. In H0, simulated N* values do not deviate from zero. In H1, N* is consistently positive. As already seen in Figure 4, neither of the two models produces large enough nutrient concentrations in deep waters. N* in H2 qualitatively approaches the observed pattern, but maximum nutrient concentrations in deep waters remain too low. Model H3, where heterotrophic diazotrophs co-exist with colonial and unicellular autotrophic diazotrophs, is best able to replicate the range of NO_3 and PO_4 concentrations and the pattern of N*, although N* is lower than observed especially at high nutrient concentrations.

Figure 6 f-h shows results from three of the four additional model versions based on H3 (H3a, H3c and H3d), in which autotrophic diazotrophs were sequentially removed from the model. In addition to heterotrophic diazotrophs, model H3a includes only the colonial autotrophs. Its results are closest to H3, but show lower maximum nutrient concentrations. H3d, the model without autotrophic diazotrophs, has the narrowest range of nutrient concentrations. Results from H3b are similar to H3d due to low total nitrogen fixation rates, and are not shown.

4.2.3 Effect of N_2 Fixation on Chlorophyll and O_2

Figure 7 shows simulated and observed chlorophyll and dissolved oxygen values. The seasonal variability of total chlorophyll concentrations is reproduced well by all models, with higher chlorophyll between November and April. During these months, simulated chlorophyll concentrations are homogeneous down to 200 m. In 2007 and 2008, chlorophyll concentrations of ~0.13 mg m^{-3} are observed in the measurements reaching as deep as 500 m. This feature is also captured well by our models, as is the location of the deep chlorophyll maximum (DCM) at ~80 m between March and October. However, there are some discrepancies between model results and observations. The models overestimate spring bloom peak concentrations in 2007 and predict peak timing two months earlier than observed in 2008. Model H0 tends to underestimate

chlorophyll concentrations from the surface to the DCM during summer months. As chlorophyll concentrations are extremely low during this time of the year, these model-data differences are on the order of 0.05 to 0.1 mg m^{-3}. These discrepancies during summer months are corrected in the models with N_2 fixation.

Simulated oxygen concentrations exhibit larger differences between models and observations, in particular below the mixed layer, where air-sea fluxes do not directly affect oxygen concentrations. Model versions without diazotrophs (H0 and H0') show similar deep-oxygen variability, with a small underestimation of oxygen during the winter of 2007, and a small overestimation after the winter of 2008. Model re-calibration for the model versions with diazotrophs results in changes in deep oxygen. H1, the model with generic diazotrophs, exhibits the largest model-observation misfits. As in the case of deep NO_3, the best deep-oxygen representation is obtained with H3.

4.2.4 Validation against Independent Observations

Observations from 2010 to 2014 (outside the optimization period) are used to independently validate the models. The root-mean-square errors (RMSEs) in Table 4 show that, in terms of chlorophyll, PO_4 and surface O_2, all models behave similarly and achieve similar agreement for assimilated and independent observations. As demonstrated in the previous sections, the model versions mainly diverge in their behaviour with respect to NO_3, with some differences in O_2 concentrations. Between 0 and 100 m, H3 has the largest RMSEs for NO_3, but below 100 m it has the lowest values, particularly against unassimilated NO_3. H3 also has the lowest RMSEs for surface and deep oxygen (Table 4).

Figure 8 shows observed and simulated NO_3 inventories in 0 – 100 m and below 100 m outside the assimilation period. Compared against the other model versions, H3 increasingly overestimates surface NO_3 over time. However, the deep NO_3 inventory is best represented by H3. By the end of the observed time series, between 2013 and 2014, H3 starts to also overestimate deep NO_3.

4.2.5 Primary Production and N_2 Fixation Rates

We now compare the simulated rates of primary production with those reported for the Gulf of Aqaba by Rahav et al. (2015) and Iluz et al. (2009) (Figure 9a) and the simulated rates of N_2 fixation with those measured by Rahav et al. (2015) and Foster et al., (2009) (Figure 9b). Following Rahav et al. (2015), we show the rates at the DCM and their averages above and below the DCM. The depth-resolved in situ primary production rates reported by Iluz et al. (2009) were also averaged in the same way for comparison. Where necessary, primary production in carbon units was converted to the model's nitrogen units using the Redfield ratio.

Simulated primary production above the DCM ranges from 0.02 to 0.85 mmol N m^{-3} d^{-1}, and exhibits an annual cycle with peaks of productivity in October and April. A prolonged period of low primary production extends from April to September in most model versions. Model versions H3b and H3d maintain rates twice as large as the rest of the models during the

summer/fall period. Aside from H3b and H3d, differences between models are small and simulated rates agree with those measured by Iluz et al. (2009) and Rahav et al. (2015).

Above the DCM, models H1, H2, H3 and H3a show a well-defined N_2 fixation peak during summer months (i.e., after the peak in primary production). Maximum rates in these models range from 0.001 to 0.1 mmol N m^{-3} d^{-1}, which agrees with the observed rates by Foster et al. (2009) and Rahav et al. (2015). In general, simulated N_2 fixation rates are low during winter and spring. Similar temporal patterns and differences between model versions occur at the DCM and below. Peaks in N_2 fixation at these depth levels occur after the surface peak, and have a shorter duration and smaller amplitude. Deep N_2 fixation rates estimated by models without heterotrophic diazotrophs do not match the observed rates by Rahav et al. (2015).

5 Discussion

5.1 Is N_2 Fixation Relevant in the Gulf of Aqaba?

In this study we implemented and optimized models with different assumptions about N_2 fixation in the Gulf of Aqaba. The models range from one neglecting N_2 fixation to another assuming that, in addition to two autotrophic diazotroph groups, heterotrophic N_2 fixation can occur in the entire water column (i.e., independent of light availability). While the models are very similar in their abilities to replicate chlorophyll and PO_4, model H3 performed the best in reproducing the observed pattern of deep-NO_3 accumulation and O_2. The models' levels of performance at replicating vertical NO_3 distributions also affect their ability to reproduce N*. When we neglect N_2 fixation, excess phosphate tends to dominate the whole water column, contrary to the observations. Explicitly accounting for N_2 fixation (H1, H2, H3) improves the models' abilities to replicate N* variability and vertical structure. The best model performance was obtained with two groups of autotrophic organisms and a group of heterotrophic organisms (H3). A model without explicit N_2 fixation, but in the absence of sediment denitrification, also increases the accumulation of deep NO_3 in a similar fashion as version H2. In the models with denitrification, the average sediment denitrification flux is 0.25 ± 0.46 mmol N m^{-2} d^{-1}, with a maximum value of 3.01 mmol N m^{-2} d^{-1}. These values at are the lower end of a global compilation of sediment denitrification rates by Fennel et al. (2009), which have a mean of 2.2 mmol N m^{-2} d^{-1} and maximum values exceeding 10 mmol N m^{-2} d^{-1}.

The excess nitrogen observed in the Gulf of Aqaba is in contrast to exterior waters from the Arabian Sea and Indian Ocean, which are considered net nitrogen sink regions (Gruber and Sarmiento, 1997). It has been hypothesized that limited deep-water exchange at Bab-el-Mandeb allows waters of the Red Sea outside of the Gulf of Aqaba to acquire different characteristics from inflowing Arabian Sea waters (Naqvi et al., 1986). Our model results support this hypothesis and suggest that N_2 fixation is key for the formation of the distinct biochemical characteristics in the Gulf of Aqaba.

There are too few reported values of dissolved inorganic nitrogen-to-phosphorus ratios for the Red Sea region from Bab-el-Mandeb to the Strait of Tiran to provide a complete idea of the spatial distribution of N*; however, the limited available information supports our conclusions. From Naqvi et al.'s (1986) observations we calculate excess nitrogen of N* = +2.5 mmol m^{-3} in sub-surface waters outflowing at the Bab-el-Mandeb towards the Arabian Sea (reported as N:P ratios of 21).

They inferred that N_2 fixation is a process required to account for the anomalies in the nitrogen budget between incoming and outgoing waters at Bab-el-Mandeb. N* values in the Red Sea are significantly higher than those of the Arabian Sea and Indian Ocean, where a strong deficit of nitrogen develops as losses due to denitrification exceed the input of newly fixed nitrogen (Burkill et al., 1993; Naqvi, 1994; Gruber and Sarmiento, 1997; Morrison et al., 1998, 1999). Close to the entrance of the Persian Gulf, N* values are below -5 mmol m^{-3} at all depths and seasons reported, with minimum excess phosphate values on the order of -8 mmol m^{-3} (Gruber and Sarmiento, 1997).

The lowest negative N* values observed in surface waters in the Gulf of Aqaba during summer are not fully captured by any of our model versions; however this is not a source of large data-model discrepancies. In the context of a one-dimensional framework, we cannot reject the possibility that these low N* values are a remnant signal of denitrification in the Arabian Sea. Considering the regional characteristics, our models suggest that, despite low N_2 fixation rates, this process is necessary to explain positive N* values in the Gulf of Aqaba, and the interannual accumulation of deep nitrate during years with weak convection.

5.2 How does N_2 fixation Contribute to Primary Production?

In this section we discuss the contribution of N_2 fixation to primary production in the Gulf of Aqaba, and our quantitative estimates of N_2 fixation with respect to global rates (Figures 9-10). Our estimates of surface primary productivity agree with those reported by Iluz et al. (2009) for March-April of 2008. However, our models overestimate surface primary productivity values in 2010 when compared to those reported by Rahav et al. (2015). On average, our best-performing model versions yield annual primary production rates of 304±56.9 g C m^{-2} yr^{-1} (H3) and 277±82.5 g C m^{-2} yr^{-1} (H3a). These rates are higher than previously published annual averages, which range from 80 g C m^{-2} y^{-1} (Levanon-Spanier et al., 1979) to 170 g C m^{-2} y^{-1} (Iluz, 1991), whereas more recent unpublished primary production estimates at IUI range between 141 and 197 g C m^{-2} y^{-1} (pers. comm. Y. Shaked).

The ratio of new to total primary production (f-ratio) in our experiments ranges from 15% to 80%. Maximum f-ratios are estimated in January and February due to significant contributions from deep NO_3, whereas f-ratios are at their minimum during stratified conditions (June – August). Our best-performing model version, H3, estimates a summer minimum f-ratio 0.22. The average f-ratio for all scenarios is 0.47. This agrees with published estimates for the Gulf of Aqaba of 0.5 during the stratified period as determined from a nitrate-diffusion model (Badran et al., 2005).

Total annual N_2 fixation rates from our best-performing model versions (H3 and H3a) are similar to high estimates reported for other regions (Capone and Carpenter, 1982; Michaels et al., 1996; Lee et al., 2002), while those obtained in the other model experiments are within the range of values reported for the Gulf of Aqaba. The intensity of winter mixing has a minor effect on N_2 fixation rates; the largest effect occurred in H3a where N_2 fixation increased by 15% after deep winter mixing. Based on our best-performing model version (H3), we estimate that 10% to 14% of the total primary production is supported by N_2 fixation.

Biogeosciences Discuss., https://doi.org/10.5194/bg-2017-550
Manuscript under review for journal Biogeosciences
Discussion started: 19 January 2018

5.3 Are Heterotrophic N_2 Fixers Important?

In contrast to previous models (e.g., Hood et al., 2001; Fennel et al., 2002; Monteiro et al., 2010; Moore et al., 2004), our model version H3 relaxes the assumption of light dependence for diazotrophy, through the inclusion of heterotrophic diazotrophs in addition to two groups of autotrophic diazotrophs. This model simulates estimates of dissolved inorganic nutrients and oxygen that compare closest to the observations. A good estimate can also be obtained in the absence of unicellular autotrophic diazotrophs (H3a). All model versions with heterotrophic organisms (H3a – H3d) are able to match observed estimates of N_2 fixation in deep waters of the Gulf of Aqaba. Without heterotrophic diazotrophs, N_2 fixation rates below the DCM are underestimated.

There is growing evidence of non-cyanobacterial N_2 fixation in aphotic waters (Benavides et al., 2017; Moisander et al., 2017). For instance, N_2 fixation rates in mesopelagic and abyssopelagic waters down to 2000 m (Fernandez et al., 2011; Bonnet et al., 2013; Loescher et al., 2014) have been attributed to non-cyanobacterial organisms, including proteobacteria (Turk-Kubo et al., 2014). These nifH-expressing heterotrophic phylotypes can be as abundant as unicellular cyanobacterial groups and dominate the deep and dark zones of the water column (Church et al. 2005; Langlois et al., 2005; Riemann et al., 2010). Genetic evidence and rate estimates from the Gulf of Aqaba suggest that nifH expressing heterotrophic proteobacteria α and γ may explain the correlation of bacterial productivity rates with N_2 fixation rates (Rahav et al., 2013; 2015). Aside from the Gulf of Aqaba, aphotic N_2 fixation and nifH gene expression have also been reported in the Baltic Sea (Farnelid et al., 2013), Arabian Sea (Jayakumar et al., 2012) and Mediterranean Sea (Rahav et al., 2013).

Despite the importance of heterotrophic diazotrophs in our model, the simulated colonial diazotroph blooms are responsible for the highest N_2 fixation rates, so they are a necessary model aspect to achieve resemblance with the observed N* patterns and deep oxygen. This is in line with evidence of extensive blooms of *Trichodesmium spp.* being responsible for the high N_2 fixation rates observed in the Arabian Sea and Red Sea (Capone et al., 1998; Post et al., 2002; Foster et al., 2009). In the northern Gulf of Aqaba, colonies and free trichomes of *Trichodesmium spp.* are found throughout the year down to a 100 m depth (Post et al., 2002). Ephemeral blooms of *T. erythraeum* and *T. thiebautii* have been documented near the coast of Eilat (Post et al., 2002, Gordon et al., 1994; Kimor and Golandsky, 1977); however, massive blooms are typically absent (Foster et al., 2009; Mackey et al., 2007). As new observational information is collected, further model refinements may be necessary to better reflect the actual contribution of different diazotrophic groups in the Gulf of Aqaba.

Our different model versions provide insights into possible effects of competition between diazotrophs, although results are not completely intuitive. For instance, when there are fewer competitors for the phosphorus resources, N* becomes skewed towards excess of nitrogen, but neither NO_3 nor PO_4 reach their maximum concentrations (Figure 8). This is a result of abundant nitrate and ammonium in mid-depth waters, and depleted phosphate throughout the whole water column. In general, our results suggest that including at least one autotrophic and one heterotrophic diazotroph group is necessary to capture surface and deep-water biochemical patterns.

5.4 Limitations and Uncertainties

The one-dimensional nature of our physical setting, which neglects the contribution of horizontal advection to the vertical structure of simulated tracers, can be considered a limitation of this study. This simplification is, however, necessary to perform model calibration and test multiple model structures at a manageable computational expense. We applied temperature and salinity nudging to ensure accurate representation of the vertical density structure. Comparison of the simulated vertical structure with and without nudging shows that this correction has negligible effects on deep waters, where the effects of N_2 fixation are the most relevant. This is consistent with the existing literature about circulation of the Gulf of Aqaba, which describes how geomorphology and bathymetry limit water exchange between the Gulf of Aqaba and the Red Sea to the upper 300 m (Wolf-Vecht et al., 1992; Biton and Gildor, 2011). It is, therefore, unlikely that horizontal transport could explain the observed accumulation of deep NO_3.

An intrinsic limitation of all functional-type biological models is the uncertainty associated with parameter values (Denman, 2003). We reduced this uncertainty by using systematic parameter optimization. This allows for a more objective comparison of different model structures and is preferable to subjective tuning. Nonetheless, parameters related to the diazotrophs are unconstrained by the observations and instead follow the observational and laboratory literature. Given these uncertainties, we opted for teasing apart the effects of mechanistic assumptions rather than modifying diazotrophs behaviour through the parameter values.

6 Conclusions

We implemented and optimized biogeochemical models that represent a range of different assumptions about diazotrophy in a 700 m-deep pelagic station from the northern Gulf of Aqaba. Our model results demonstrate the importance of N_2 fixation in replicating the observed water-column-integrated nitrogen inventories. The model without N_2 fixation is unable to replicate the observed vertical structure of inorganic nitrogen and phosphorus. The models that include diazotrophs significantly modify these variables by increasing the fraction of remineralized nitrogen from organic matter decomposition. Oxygen distributions are also affected by these changes. Additional deep-oxygen consumption occurs in the models with N_2 fixation due to increased organic matter decomposition, which better resembles the observations. The observed vertical structure of nutrient ratios and oxygen is reproduced best with a model that includes heterotrophic, and colonial and unicellular autotropic diazotrophs suggesting that heterotrophic N_2 fixation is necessary to explain the observed excess nitrogen at this location. The N_2 fixation rates simulated by this model are similar to the highest observational estimates from the Gulf of Aqaba. Aphotic N_2 fixation is simulated to occur at lower rates than maximum autotrophic N_2 fixation, but occurs continuously over a large portion of the water column. This suggests that heterotrophic diazotrophs set a background rate of N_2 fixation in the ocean that should be considered further in global estimates and biogeochemical models.

Acknowledgements We thank the Inter University Institute for Marine Sciences in Eilat and A. Genin for providing the observational data, and E. Landou, B. Lazar, S. Kienast, H. Gildor, E. Boss, A. Torfstein, and M. Lewis for insightful discussions. We gratefully acknowledge financial support from the Schulich Marine Studies Initiative to KF, IBF, and BL.

References

Amon, R.M.W. and Benner, R.: Photochemical and microbial consumption of dissolved organic carbon and dissolved oxygen in the Amazon River system, Geochimica et Cosmochimica Acta, 60, 10, 1783-1792, 1996.

Badran, M.I., Rasheed, M., Manasrah, R. and Al-Najjar, T.: Nutrient flux fuels the summer primary productivity in the oligotrophic waters of the Gulf of Aqaba, Red Sea, Oceanologia 47, 1, 2005.

Ben-Sasson, M., Brenner, S. and Paldor, N.: Estimating air–sea heat fluxes in semienclosed basins: The case of the Gulf of Elat (Aqaba), J. Phys. Oceanogr., 39, 185–202, 2009.

Berman, T., Paldor, N. and Brenner, S.: The seasonality of tidal circulation in the Gulf of Elat, Isr. J. Earth Sci., 52, 2003.

Berman, T., Paldor, N. and Brenner, S.: Simulation of wind-driven circulation in the Gulf of Elat (Aqaba), J. Mar. Syst., 26, 349–365. doi:10.1016/S0924-7963(00)00045-2, 2000.

Berman-Frank, I., Cullen, J.T., Shaked, Y., Sherrell, R.M. and Falkowski, P.G.: Iron availability, cellular iron quotas, and nitrogen fixation in Trichodesmium, Limnol. Oceanogr., 46, 1249–1260, 2001.

Biton, E., Silverman, J. and Gildor, H.: Observations and modeling of a pulsating density current, Geophys. Res. Lett., 35, 14, 2008.

Biton, E. and Gildor, H.: The general circulation of the Gulf of Aqaba (Gulf of Eilat) revisited: The interplay between the exchange flow through the Straits of Tiran and surface fluxes, J. Geophys. Res., 116, C8, doi:10.1029/2010JC006860, 2011.

Bonnet, S., Bethelot, H., Turk-Kubo, K., Fawcett, S., Rahav, E., L'Helguen, S. and Berman-Frank, I.: Dynamics of N_2 fixation and fate of diazotroph-derived nitrogen in a low-nutrient, low-chlorophyll ecosystem: results from the VAHINE mesocosm experiment (New Caledonia), Biogeosciences, 13, 2653–2673. doi:10.5194/bg-13-2653-2016, 2016.

Bonnet, S., Dekaezemacker, J., Turk-Kubo, K.A., Moutin, T., Hamersley, R.M., Grosso, O., Zehr, J.P. and Capone, D.G.: Aphotic N_2 fixation in the eastern tropical South Pacific Ocean, PloS one, 8, 12, e81265, 2013.

Burchard, H., Bolding, K. and Villarreal, M.: GOTM- a general ocean turbulence model. Theory, applications and test cases (Technical Report No. EUR 18745 EN), European Commission, 1999.

Burkill, P.H., Mantoura, R.F.C. and Owens, N.J.P.: Biogeochemical cycling in the northwestern Indian Ocean: a brief overview, Deep Sea Res. Part II Top. Stud. Oceanogr., 40, 643–649, 1993.

Capone, D.G., Burns, J.A., Montoya, J.P., Subramaniam, A., Mahaffey, C., Gunderson, T., Michaels, A.F. and Carpenter, E.J.: Nitrogen fixation by *Trichodesmium spp.*: An important source of new nitrogen to the tropical and subtropical North Atlantic Ocean, Glob. Biogeochem. Cycles, 19, 2, 2005.

Capone, D.G. and Carpenter, E.J.: Nitrogen fixation in the marine environment, Science, 217, 1140–1142, 1982.

Capone, D.G., Subramaniam, A., Montoya, J.P., Voss, M., Humborg, C., Johansen, A.M., Siefert, R.L. and Carpenter, E.J.: An extensive bloom of the N_2-fixing cyanobacterium *Trichodesmium erythraeum* in the central Arabian Sea, Mar. Ecol. Prog. Ser., 172, 281–292, 1998.

Capone, D.G., Zehr, J.P., Paerl, H.W., Bergman, B. and Carpenter, E.J.: Trichodesmium, a globally significant marine cyanobacterium, Science, 276, 1221–1229, 1997.

Carlson, D.F., Fredj, E. and Gildor, H.: The annual cycle of vertical mixing and restratification in the Northern Gulf of Eilat/Aqaba (Red Sea) based on high temporal and vertical resolution observations, Deep Sea Res. Part Oceanogr. Res. Pap., 84, 1–17, 2014.

Carlson, D.F., Fredj, E., Gildor, H., Biton, E., Steinbuck, J.V., Monismith, S.G. and Genin, A.: Observations of tidal currents in the northern Gulf of Eilat/Aqaba (Red Sea), J. Mar. Syst., 102, 14–28, 2012.

Carpenter, E.J. and McCarthy, J.J.: Nitrogen fixation and uptake of combined nitrogenous nutrients by Oscillatoria (Trichodesmium) thiebutii in the western Sargasso Sea, Limnol. Oceanogr., 20, 389–401, 1975.

Carpenter, E.J., Montoya, J.P., Burns, J.A., Mulholland, M.R. and Subramaniam, A., Capone, D.G.: Extensive bloom of a N_2-fixing diatom/cyanobacterial association in the tropical Atlantic Ocean, Mar. Ecol. Prog. Ser., 185, 273–283, 1999.

Carpenter, E.J. and Roenneberg, T.: The marine planktonic cyanobacteria *Trichodesmium spp.*: photosynthetic rate measurements in the SW Atlantic Ocean, Mar. Ecol. Prog. Ser., 267–273, 1995.

Chase, Z., Paytan, A., Johnson, K.S., Street, J. and Chen, Y.: Input and cycling of iron in the Gulf of Aqaba, Red Sea, Glob. Biogeochem. Cycles, 20, 3, 2006.

Chen, Y., Mills, S., Street, J., Golan, D., Post, A., Jacobson, M. and Paytan, A.: Estimates of atmospheric dry deposition and associated input of nutrients to Gulf of Aqaba seawater, J. Geophys. Res. Atmosphere, 112, D4, 2007.

Church, M.K., Jenkinks, Bethany D., Karl, D.M. and Zehr, J.: Vertical distributions of nitrogen-fixing phylotypes at Stn ALOHA in the oligotrophic North Pacific Ocean. Aquat. Microb. Ecol. 38, 3–14, 2005.

Denman, K.L.: Modelling planktonic ecosystems: parameterizing complexity, Prog. Oceanogr., 57, 429–452, 2003.

Deutsch, C., Sigman, D.M., Gruber, N. and Dunne, J.P.: Spatial coupling of nitrogen inputs and losses in the ocean, Nature, 445, 163–168. doi:10.1038/nature05392, 2007.

Dutkiewicz, S., Ward, B.A., Monteiro, F.M. and Follows, M.: Interconnection nitrogen fixers and iron in the Pacific Ocean: Theory and numerical simulations, Glob. Biogeochem. Cycles, 26, 1, 2012.

Dutkiewicz, S., Morris, J., Follows, M.J., Scott, J., Levitan, O., Dyhrman, S.T. and Berman-Frank, I.: Impact of ocean acidification on the structure of future phytoplankton communities, Nature Climate Change, 5, 11, 1002-1006, doi: 10.1038/NCLIMATE2722, 2015.

Enríquez, S.C.M.D., Duarte, C.M. and Sand-Jensen, K.A.J.: Patterns in decomposition rates among photosynthetic organisms: the importance of detritus C: N: P content, Oecologia, 94, 4, 457-471, 1993.

Eppley, R.W. and Peterson, B.J.: Particulate organic matter flux and planktonic new production in the deep ocean, Nature, 282, 677, 1979.

Falkowski, P.G.: Evolution of the nitrogen cycle and its influence on the biological sequestration of CO_2 in the ocean, Nature, 387, 272–274, 1997.

Fahnenstiel, G.L., McCormick, M.J., Lang, G.A., Redalje, D.G., Lohrenz, S.E., Markowitz, M., Wagoner, B. and Carrick, H.J.: Taxon-specific growth and loss rates for dominant phytoplankton populations from the northern Gulf of Mexico, Mar. Ecol. Prog. Ser., Oldendorf ,117, 1, 229-239, 1995.

Farnelid, H., Bentzon-Tilia, M., Andersson, A.F., Bertilsson, S., Jost, G., Labrenz, M., Jürgens, K. and Riemann, L.: Active nitrogen-fixing heterotrophic bacteria at and below the chemocline of the central Baltic Sea, The ISME Journal, 7, 1413–1423, doi:10.1038/ismej.2013.26, 2013.

Fennel, K., Brady, D., DiToro, D., Fulwiler, R.W., Gardner, W.S., Giblin, A., McCarthy, M.J., Rao, A., Seitzinger, S., Thouvenot-Korppoo, M. and Tobias, C.: Modeling denitrification in aquatic sediments, Biogeochemistry, 93, 159–178, 2009.

Fennel, K., Follows, M. and Falkowski, P.G.: The co-evolution of the nitrogen, carbon and oxygen cycles in the Proterozoic, Ocean. Am. J. Sci., 305, 526-545, 2005.

Fennel, K., Hu, J., Laurent, A., Marta-Almeida, M. and Hetland, R.: Sensitivity of hypoxia predictions for the northern Gulf of Mexico to sediment oxygen consumption and model nesting, J. Geophys. Res. Oceans, 118, 990–1002, 2013.

Fennel, K., Spitz, Y.H., Letelier, R. and Abbott, M.R.: A deterministic model for N_2 fixation at stn. ALOHA in the subtropical North Pacific Ocean, Deep-Sea Res. II, 49, 149–174, 2002.

Fennel, K., Wilkin, J., Levin, J., Moisan, J., O'Reilly, J.E. and Haidvogel, D.: Nitrogen cycling in the Middle Atlantic Bight: Results from a three-dimensional model and implications for the North Atlantic nitrogen budget, Glob. Biogeochem. Cycles 20, 14, doi:10.1029/2005GB002456, 2006.

Fennel, K., Losch, M., Schröter, J., and Wenzel M.: Testing a marine ecosystem model: Sensitivity analysis and parameter optimization, J. Mar. Syst., 28, 1, 45-63, 2001.

Foster, R.A., Paytan, A. and Zehr, J.P.: Seasonality of N_2 fixation and nifH gene diversity in the Gulf of Aqaba (Red Sea), Limnol. Oceanogr., 54, 219–233, 2009.

Fuller, N.J., West, N.J., Marie, D., Yallop, M., Rivlin, T., Post, A.F. and Scanlan, D.J.: Dynamics of community structure and phosphate status of picocyanobacterial populations in the Gulf of Aqaba, Red Sea, Limnol. Oceanogr., 50, 363–375, 2005.

Geider, R.J., MacIntyre, H.L. and Kana, T.M.: Dynamic model of phytoplankton growth and acclimation: responses of the balanced growth rate and the chlorophyll a: carbon ratio to light, nutrient-limitation and temperature, Mar. Ecol. Prog. Ser., 148, 187–200, 1997.

Gifford, D.J., Fessenden, L.M., Garrahan, P.R. and Martin, E.: Grazing by microzooplankton and mesozooplankton in the high-latitude North Atlantic Ocean: Spring versus summer dynamics, J. of Geophys. Res. Oceans, 100, C4, 6665-6675, 1995.

Genin, A. and Paldor, N.: Changes in the circulation and current spectrum near the tip of the narrow, seasonally mixed Gulf of Elat, Isr. J. Earth. Sci., 47, 87–92, 1998.

Gordon, N., Angel, D.L., Neori, A., Kress, N. and Kimor, B.: Heterotrophic dinoflagellates with symbiotic cyanobacteria and nitrogen limitation in the Gulf of Aqaba, Mar. Ecol. Prog. Ser., 83–88, 1994.

Gregg, W.W.: Assimilation of SeaWiFS ocean chlorophyll data into a three-dimensional global ocean model, J. Mar. Syst., 69, 205–225, 2008.

Gruber, N. and Galloway, J.N.: An Earth-system perspective of the global nitrogen cycle, Nature, 451, 293–296, 2008.

Gruber, N. and Sarmiento, J.L.: Global patterns of marine nitrogen fixation and denitrification, Glob. Biogeochem. Cycles, 11, 235–266, 1997.

Haug, G.H., Pedersen, T.F., Sigman, D.M., Calvert, Nielsen, B. and Peterson, L.C.: Glacial/interglacial variations in production in nitrogen fixation in the Cariaco Basin during the last 580 kyr, Paleoceanography, 13, 427–432, 1998.

Hood, R., Bates, N.R., Capone, D.G. and Olson, D.B.: Modeling the effect of nitrogen fixation on carbon and nitrogen fluxes BATS, Deep-Sea Res. II, 48, 1609–1648, 2001.

Houck, C.R., Joines, J.A. and Kay, M.G.: A genetic algorithm for function optimization: A Matlab implementation (Technical Report No. NCSU-IE-TR-95-09), North Carolina State University, Raleigh, NC, 1995.

Hutchins, D.A., Fu, F.-X., Zhang, Y., Warner, M.E., Feng, Y., Portune, K., Bernhardt, P. and Mullholland, M.R.: CO_2 control of Trichodesmium N_2 fixation, photosynthesis, growth rates, and elemental ratios: Implications for past, present, and future ocean biogeochemistry, Limnol. Oceanogr., 52, 1293–1304, 2007.

Iluz, D.: Primary production of phytoplankton in the northern Gulf of Eilat, Red Sea, MSc thesis, Bar-Ilan University, Ramat-Gan (in Hebrew with English abstract), 1991.

Iluz, D., Dishon, G., Capuzzo, E., Meeder, E., Astoreca, R., Montecino, V., Znachor, P., Ediger, D. and Marra, J.: Short-term variability in primary productivity during a wind-driven diatom bloom in the Gulf of Eilat (Aqaba), Aquat. Microb. Ecol., 56, 205–215, 2009.

Karl, D.: Nutrient dynamics in the deep blue sea, TRENDS Microbiol., 10, 410–418, 2002.

Jayakumar, A., Al-Rshaidat, M.M.D., Ward, B.B. and Mulholland, M.R.: Diversity, distribution, and expression of diazotroph nifH genes in oxygen-deficient waters of the Arabian Sea FEMS Microbiology Ecology, 82, 3, 597–606,https://doi.org/10.1111/j.1574-6941.2012.01430.x, 2012.

Kerbrat, A.S., Darius, H.T., Pauillac, S., Chinain, M., and Laurent, D.: Detection of ciguatoxin-like and paralysing toxins in *Trichodesmium* spp. from New Caledonia lagoon, Mar. Pollut. Bull., 2010, 61, 360–366, 2010.

Kerbrat, A.S., Amzil, Z., Pawlowiez, R., Golubic, S., Sibat, M., Darius, H.T, Chinain, M. and Laurent, D.: First Evidence of Palytoxin and 42-Hydroxy-palytoxin in the Marine Cyanobacterium *Trichodesmium.*, Mar. Drugs, 9, 543-560, doi:10.3390/md9040543, 2011.

Kimor, B. and Golandsky, B.: Microplankton of the Gulf of Elat: aspects of seasonal and bathymetric distribution, Mar. Biol., 42, 55–67, 1977.

Klinker, J., Reiss, Z., Kropach, C., Levanon, I., Harpaz, H., Halicz, E. and Assaf, G.: Observations on the circulation pattern in the Gulf of Elat (Aqaba), Red Sea, Isr. J. Earth Sci., 25, 85–103, 1976.

Kranz, S. A., Levitan, O., Richter, K. U., Prášil, O., Berman-Frank, I. and Rost, B.: Combined effects of CO_2 and light on the N_2-fixing cyanobacterium *Trichodesmium* IMS101: physiological responses, Plant Physiology, 154, 1, 334-345, 2010.

Kuhn, A.M., Fennel, K. and Mattern, J.P.: Model investigations of the North Atlantic spring bloom initiation, Prog. Oceanogr., 138, 176–193, 2015.

Labiosa, R.G., Arrigo, K.R., Genin, A., Monismith, S.G. and van Dijken, G.: The interplay between upwelling and deep convective mixing in determining the seasonal phytoplankton dynamics in the Gulf of Aqaba: Evidence from SeaWiFS and MODIS, Limnol. Oceanogr., 48, 2355–2368, 2003.

Landry, M.R., Hasset, R.P., Fagerness, V., Downs, J. and Lorenzen, C.J.: Effect of food acclimation on assimilation efficiency of *Calanus pacificus*, Limnol. and Oceanogra., 29, 361–364, 1984.

Lazar, B., Erez, J., Silverman, J., Rivlin, T., Rivlin, A., Dray, M., Meeder, E. and Iluz, D.: Recent environmental changes in the chemical-biological oceanography of the Gulf of Aqaba (Eilat), Aqaba-Eilat Improbable Gulf Environment, Biodiversity and Preservation, Magnes Press, Jerusalem, 49–62, 2008.

Lee, K., Karl, D.M., Wanninkhof, R. and Zhang, J., Z.: Global estimates of net carbon production in the nitrate-depleted tropical and subtropical oceans, Geophys. Res. Lett., 29, 19, 2002.

Levanon-Spanier, I., Padan, E. and Reiss, Z.: Primary production in a desert-enclosed sea-the Gulf of Elat (Aqaba), Red Sea, Deep Sea Res. Part Oceanogr. Res. Pap., 26, 673–685, 1979.

Lima, I.D. and Doney, S.C.: A three-dimensional, multinutrient, and size- structured ecosystem model for the North Atlantic, Glob. Biogeochem. Cycles, 18, 3, 2004.

Luo, Y.W., Doney, S.C., Anderson, L.A., Benavides, M., Berman-Frank, I., Bode, A., Bonnet, S., Boström, K.H., Böttjer, D., Capone, D.G. and Carpenter, E.J.: Database of diazotrophs in global ocean: abundance, biomass and nitrogen fixation rates, Earth System Science Data, 4, 1, 47-73, 2012.

Mackey, K. R., Labiosa, R. G., Calhoun, M., Street, J. H., Post, A. F., and Paytan, A.: Phosphorus availability, phytoplankton community dynamics, and taxon-specific phosphorus status in the Gulf of Aqaba, Red Sea, Limnol. and Oceanogra., 52, 2, 873-885, 2007.

Mackey, K.R., Rivlin, T., Grossman, A.R., Post, A.F. and Paytan, A.: Picophytoplankton responses to changing nutrient and light regimes during a bloom, Mar. Biol., 156, 1531–1546, 2009.

Manasrah, R., Raheed, M. and Badran, M.I.: Relationships between water temperature, nutrients and dissolved oxygen in the northern Gulf of Aqaba, Red Sea, Oceanologia, 48, 2, 2006.

Meeder, E., Mackey, K.R., Paytan, A., Shaked, Y., Iluz, D., Stambler, N., Rivlin, T., Post, A.F. and Lazar, B.: Nitrite dynamics in the open ocean-clues from seasonal and diurnal variations, Mar. Ecol. Prog. Ser., 453, 2012.

Michaels, A.F., Olson, D., Sarmiento, J.L., Ammerman, J.W., Fanning, K., Jahnke, R., Knap, A.H., Lipschultz, F. and Prospero, J.M.: Inputs, losses and transformations of nitrogen and phosphorus in the pelagic North Atlantic Ocean, in: Nitrogen Cycling in the North Atlantic Ocean and Its Watersheds, Springer, 181–226, 1996.

Moisander, P., Beinart, R.A., Hewson, I., White, A.E., Johnson, K.S., Carlson, C.A., Montoya, J.P. and Zehr, J.P.: Unicellular cyanobacterial distribution broaden the oceanic N_2 fixation domain, Science, 327, 1512–1514, 2010.

Moisander, P., Benavides, M., Bonnet, S. and Berman-Frank, I.: Chasing after Non-cyanobacterial Nitrogen Fixation in Marine Pelagic Environments, Front. Microbiol., 8, 1736, doi: https://doi.org/10.3389/fmicb.2017.01736, 2017.

Monismith, S.G. and Genin, A.: Tides and sea level in the Gulf of Aqaba (Eilat), J. Geophys. Res. Oceans, 109, 2004.

Monteiro, F.M., Follows, M. and Dutkiewicz, S.: Distribution of diverse nitrogen fixers in the global ocean, Glob. Biogeochem. Cycles, 24, 3, 2010.

Montoya, J.P., Holl, C.M., Zehr, J.P., Hansen, A., Villareal, T.A. and Capone, D.G.: High rates of N_2 fixation by unicellular diazotrophs in the oligotrophic Pacific Ocean, Nature, 420, 1027–1032, 2004.

Moore, J.K., Doney, S. and Lindsay, K.: Upper ocean ecosystem dynamics and iron cycling in a global three-dimensional model, Glob. Biogeochem. Cycles, 18, 4, 2004.

Moore, J.K., Doney, S.C., Kleypas, J.C., Glover, D.M. and Fung, I.Y.: An intermediate complexity marine ecosystem model for the global domain, Deep Sea Res., Part II, 49, 403–462, 2002.

Morrison, J.M., Codispoti, L.A., Gaurin, S., Jones, B., Manghnani, V. and Zheng, Z.: Seasonal variation of hydrographic and nutrient fields during the US JGOFS Arabian Sea Process Study, Deep Sea Res. Part II Top. Stud. Oceanogr., 45, 2053–2101, 1998.

Morrison, J.M., Codispoti, L.A., Smith, S.L., Wishner, K., Flagg, C., Gardner, W.D., Gaurin, S., Naqvi, S.W.A., Manghnani, V., Prosperie, L. and Gundersen, J.S.: The oxygen minimum zone in the Arabian Sea during 1995, Deep Sea Res. Part II Top. Stud. Oceanogr., 46, 1903–1931, 1999.

Naqvi, S.W.A.: Denitrification processes in the Arabian Sea, Proc. Indian Acad. Sci.-Earth Planet. Sci., 103, 279–300, 1994.

Naqvi, S. W. A., Hansen, H.P. and Kureishy, T.W.: Nutrient-uptake and regeneration ratios in the Red-Sea with reference to the nutrient budgets, Oceanologica acta, 9, 3, 271-275, 1986.

Nielsen, S.L.: Size-dependent growth rates in eukaryotic and prokaryotic algae exemplified by green algae and cyanobacteria: comparisons between unicells and colonial growth forms, J. Plankton Res. 28, 5, 489–498, 2006.

O'Neil, J.M. and Roman, M.R.: Ingestion of the cyanobacterium *Trichodesmium spp.* by pelagic harpacticoid copepods Macrosetella, Miracia and Oculosetella, Ecology and Morphology of Copepods, Springer, 235–240, 1994.

Pomeroy, L.R. and Wiebe, W.J.: Temperature and substrates as interactive limiting factors for marine heterotrophic bacteria, Aquat. Microb. Ecol., 23, 187–204, 2001.

Post, A. F., Dedej, Z., Gottlieb, R., Li, H., Thomas, D.N., El-Absawi, M., El-Naggar, A., El-Gharabawi, M. and Sommer, U.: Spatial and temporal distribution of *Trichodesmium spp.* in the stratified Gulf of Aqaba, Red Sea, Mar. Ecol. Prog. Ser., 239, 241–250, 2002.

Rahav, E., Bar-Zeev, E., Ohayion, S., Elifantz, H., Belkin, N., Herut, B., Mulholland, M.R. and Berman-Frank, I.R.: Dinitrogen fixation in aphotic oxygenated marine environments, Front. Microbiol., 4, 227, 2013.

Rahav, E., Herut, B., Mulholland, M.R., Belkin, N., Elifantz, H. and Berman-Frank, I.: Heterotrophic and autotrophic contribution to dinitrogen fixation in the Gulf of Aqaba, Mar. Ecol. Prog. Ser., 522, 67–77, 2015.

Riemann, L., Farnelid, H. and Steward, G.F.: Nitrogenase genes in non-cyanobacterial plankton: prevalence, diversity and regulation in marine waters, Aquat. Microb. Ecol., 61, 235-247, 2010.

Rubin, M., Berman-Frank, I. and Shaked, Y.: Dust-and mineral-iron utilization by the marine dinitrogen-fixer Trichodesmium, Nature Geoscience, 4, 8, 529-534, 2011.

Schartau, M. and Oschlies, A.: Simultaneous data-based optimization of a 1D-ecosystem model at three locations in the North Atlantic: Part I - Method and parameter estimates, J. Mar. Res., 61, 765–793, 2003.

Silverman, J. and Gildor, H.: The residence time of an active versus a passive tracer in the Gulf of Aqaba: A box model approach, J. Mar. Syst., 71, 159–170, 2008.

Smayda, T. and Bienfang, P.K., Suspension properties of various phyletic groups of phytoplankton and tintinnids in an oligotrophic, subtropical system, Mar. Ecol., 4, 289–300, 1983.

Tande, K.S. and Slagstad, D.: Assimilation efficiency in herbivorous aquatic organisms - The potential of the ratio method using 14C and biogenic silica as markers, Limnol. and Oceanogra., 30, 1093–1099, 1985.

Veldhuis, M.J.W, Timmermans, K.R., Croot, P. and van der Wagt B.: Picophytoplankton; a comparative study of their biochemical composition and photosynthetic properties, J. of Sea Res., 53, 1, 7-24, 2005.

Ward, B.A., Dutkiewicz, S., Moore, C.M. and Follows, M.: Iron, phosphorus, and nitrogen supply ratios define the biogeography of nitrogen fixation, Limnol. Oceanogr., 58, 2059–2075, 2013.

Ward, B.A., Friedrichs, M.A.M., Anderson, T.R. and Oschlies, A.: Parameter optimization techniques and the problem of underdetermination in marine biogeochemical models, J. Mar. Syst., 81, 34–43, 2010.

Wolf-Vecht, A., Paldor, N. and Brenner, S.: Hydrographic indications of advection/convection effects in the Gulf of Elat, Deep Sea Res. Part Oceanogr. Res. Pap., 39, 1393–1401, 1992.

Zarubin, M., Lindemann, Y. and Genin, A.: The dispersion-confinement mechanism: Phytoplankton dynamics and the spring bloom in a deeply-mixing subtropical sea, Prog. in Oceanogr., 155, 13-27, 2017.

Zehr, J.P.: Nitrogen fixation by marine cyanobacteria, Curr. Trends Microbiol., 19, 4, 162–173, 2011.

Zehr, J.P., Bench, S.R., Carter, B.J., Hewson, I., Niazi, F., Shi, T., Tripp, H.J. and Affourtit, J.: Globally distributed uncultivated oceanic N_2-fixing cyanobacteria lack ocygenic photosystem II, Science, 322, 1110–1112, 2008.

Zehr, J.P., Carpenter, E.J. and Villareal, T.A.: New perspectives on nitrogen-fixing microorganisms in tropical and subtropical oceans, Curr. Trends Microbiol., 8, 2, 68-73, 2000.

Zehr, J.P., Mellon, M.T. and Zani, S.: New Nitrogen-Fixing Microorganisms Detected in Oligotrophic Oceans by Amplification of Nitrogenase (nifH) Genes. Appl. Environ. Microbiol. 64, 3444–3450, 1998.

Zehr, J.P. and Ward, B.B.: Nitrogen cycling in the ocean: new perspectives on processes and paradigms. Appl. Environ. Microbiol. 68, 1015–1024, 2002.

Zehr, J.P., Waterbury, J.B., Turner, P., Montoya, J.P., Omoregie, E., Steward, G.F., Hansen, A. and Karl, D.M.: Unicellular cyanobacteria fix N_2 in the subtropical North Pacific Ocean. Nature 412, 635–637, 2001.

Biogeosciences Discuss., https://doi.org/10.5194/bg-2017-550
Manuscript under review for journal Biogeosciences
Discussion started: 19 January 2018

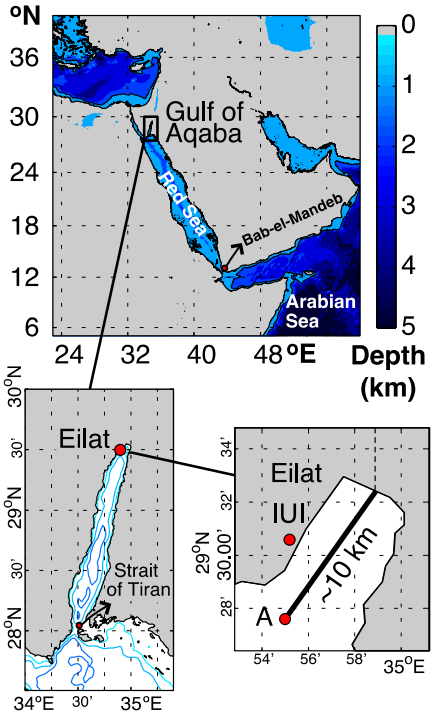

Figure 1: Map of study area showing the location of monitoring stations and geographic references.

Biogeosciences Discuss., https://doi.org/10.5194/bg-2017-550
Manuscript under review for journal Biogeosciences
Discussion started: 19 January 2018

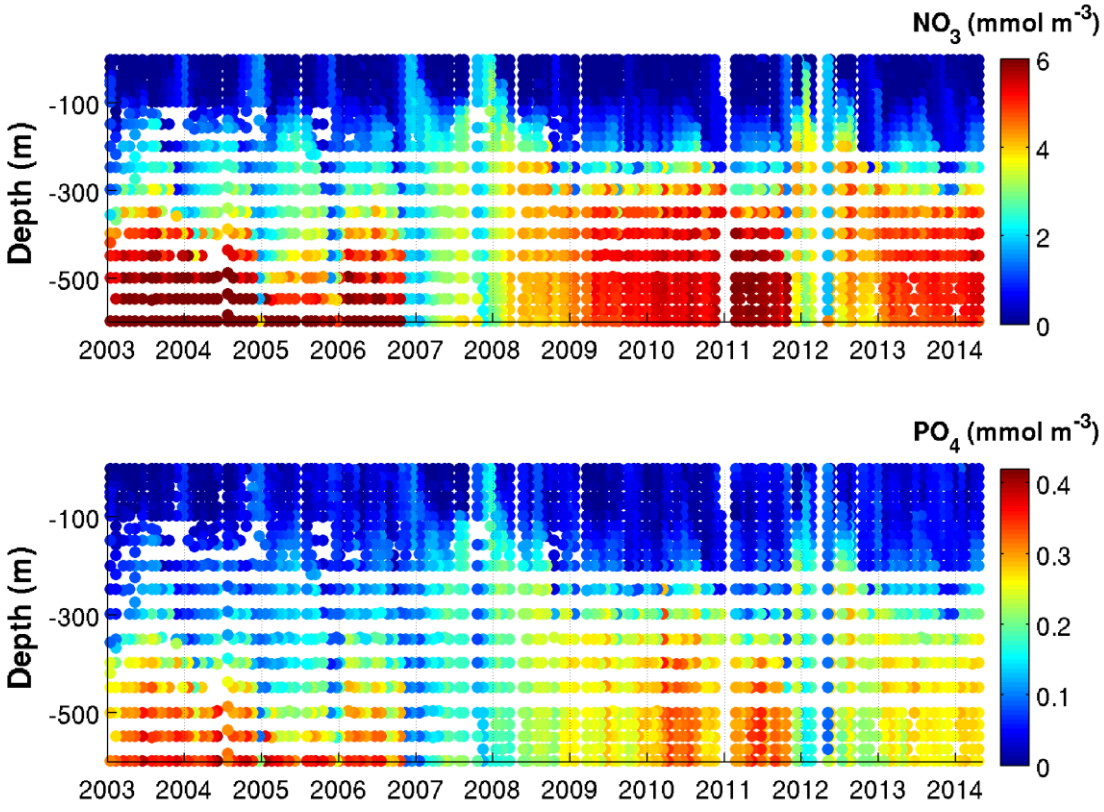

Figure 2: Vertical nitrate and phosphate distributions at Station A (Gulf of Aqaba) from 2004 to 2014. Tick marks are placed on the April 1st of every year.

Biogeosciences Discuss., https://doi.org/10.5194/bg-2017-550
Manuscript under review for journal Biogeosciences
Discussion started: 19 January 2018

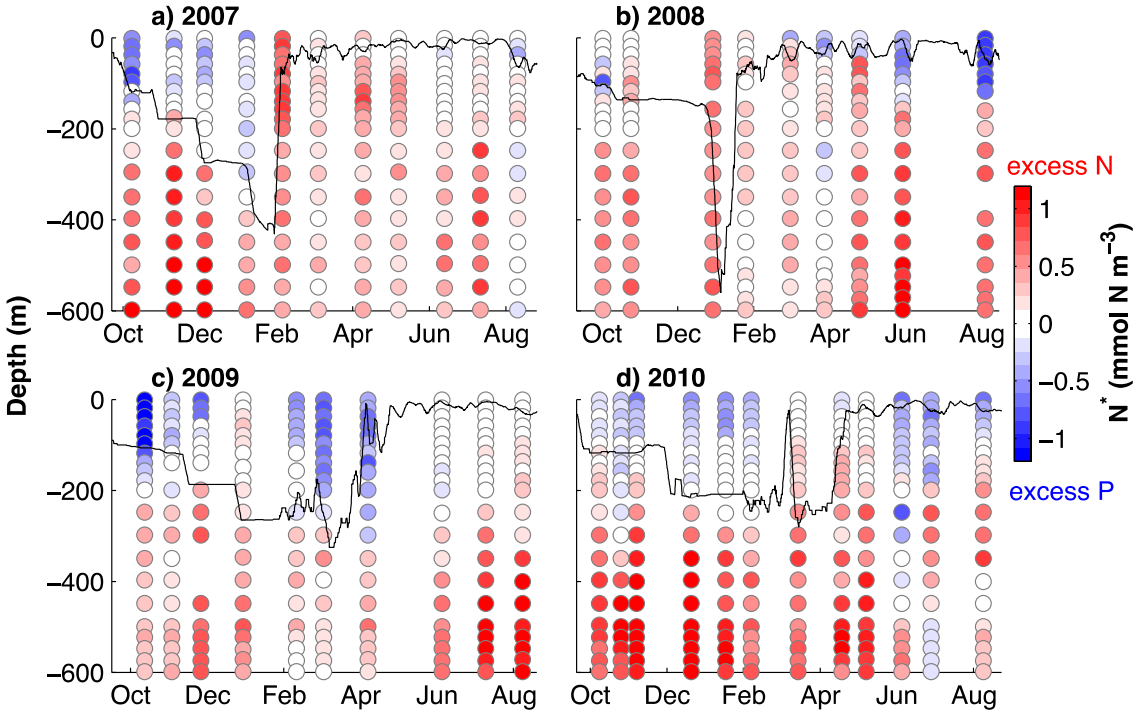

Figure 3: N* calculated from NO_3 and PO_4 profiles at Station A from Figure 2. The black lines show estimated mixed layer depths using a maximum density gradient criterion.

Biogeosciences Discuss., https://doi.org/10.5194/bg-2017-550
Manuscript under review for journal Biogeosciences
Discussion started: 19 January 2018

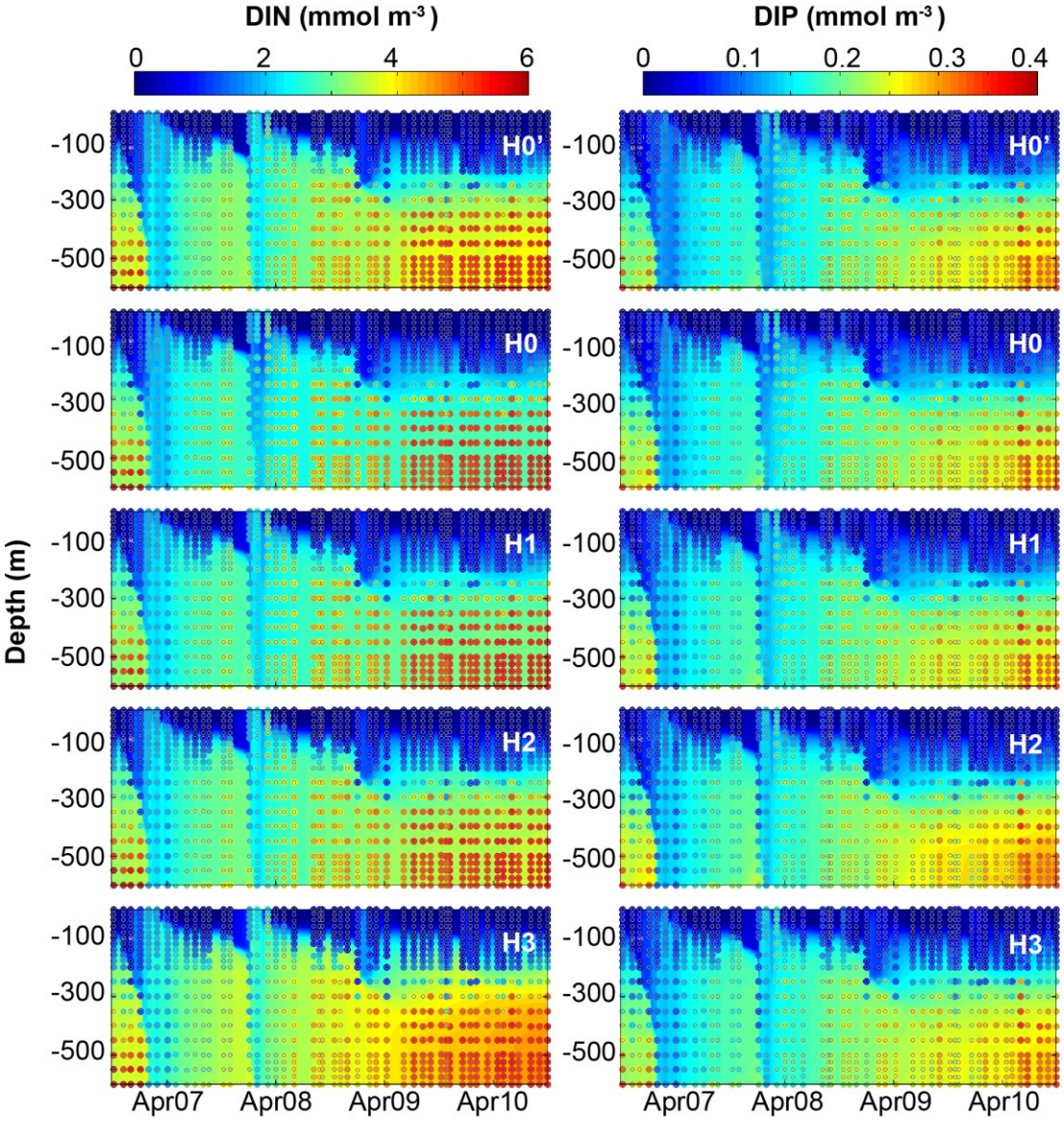

Figure 4: Observed (coloured circles) and simulated (background) NO3 and PO4 using model versions H0 (no nitrogen fixers), H1 (generic autotrophic fixer), H2 (unicellular and colonial autotrophic fixers), H3 (heterotrophic, and unicellular and colonial autotrophic fixers). The spin-up period is not shown.

Biogeosciences Discuss., https://doi.org/10.5194/bg-2017-550
Manuscript under review for journal Biogeosciences
Discussion started: 19 January 2018

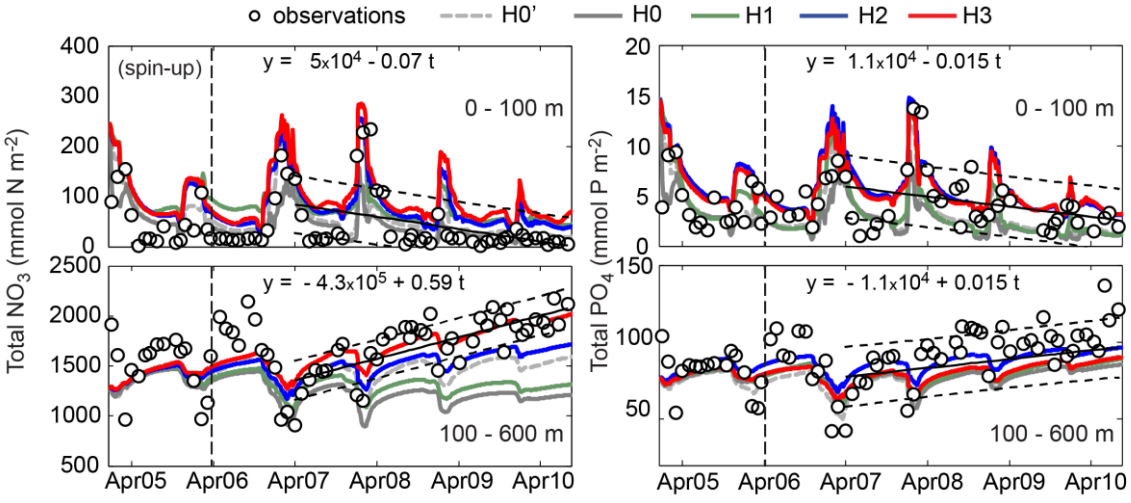

Figure 5: Observed and simulated vertically integrated NO3 and PO4 between 0 – 100 m and between 100 – 600 m using model versions H0 (no nitrogen fixers), H0' (no sediment denitrification – no fixers), H1 (generic autotrophic fixer), H2 (unicellular and colonial autotrophic fixers), H3 (heterotrophic, and unicellular and colonial autotrophic fixers).

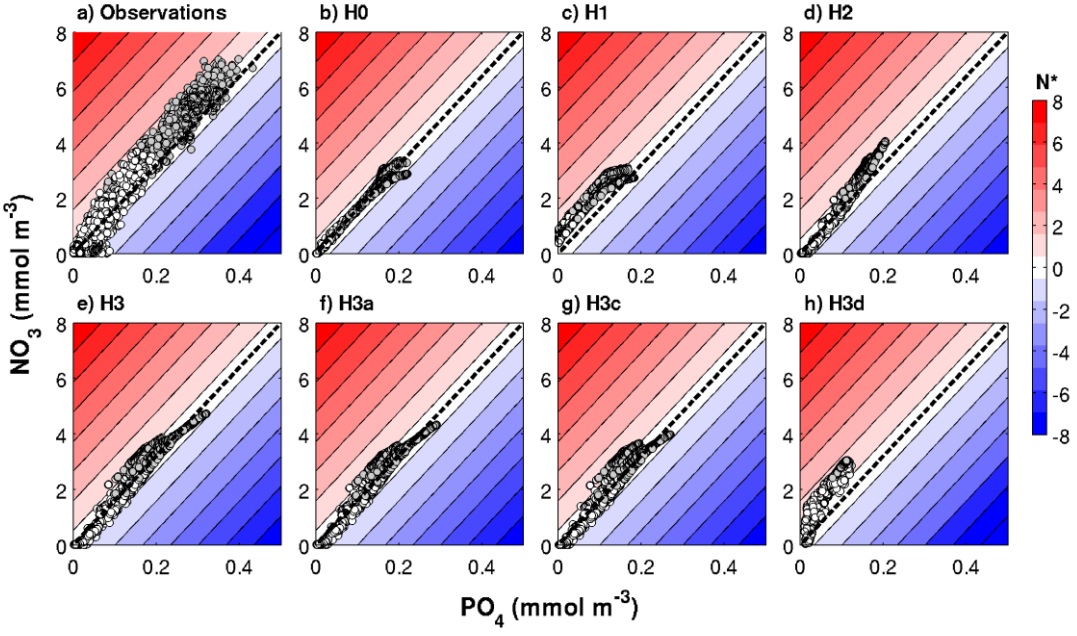

Figure 6: Observed and simulated N* range in the optimized biogeochemical models. The dashed black diagonal line marks the N* = 0, or N:P = 16 line.

Biogeosciences Discuss., https://doi.org/10.5194/bg-2017-550
Manuscript under review for journal Biogeosciences
Discussion started: 19 January 2018

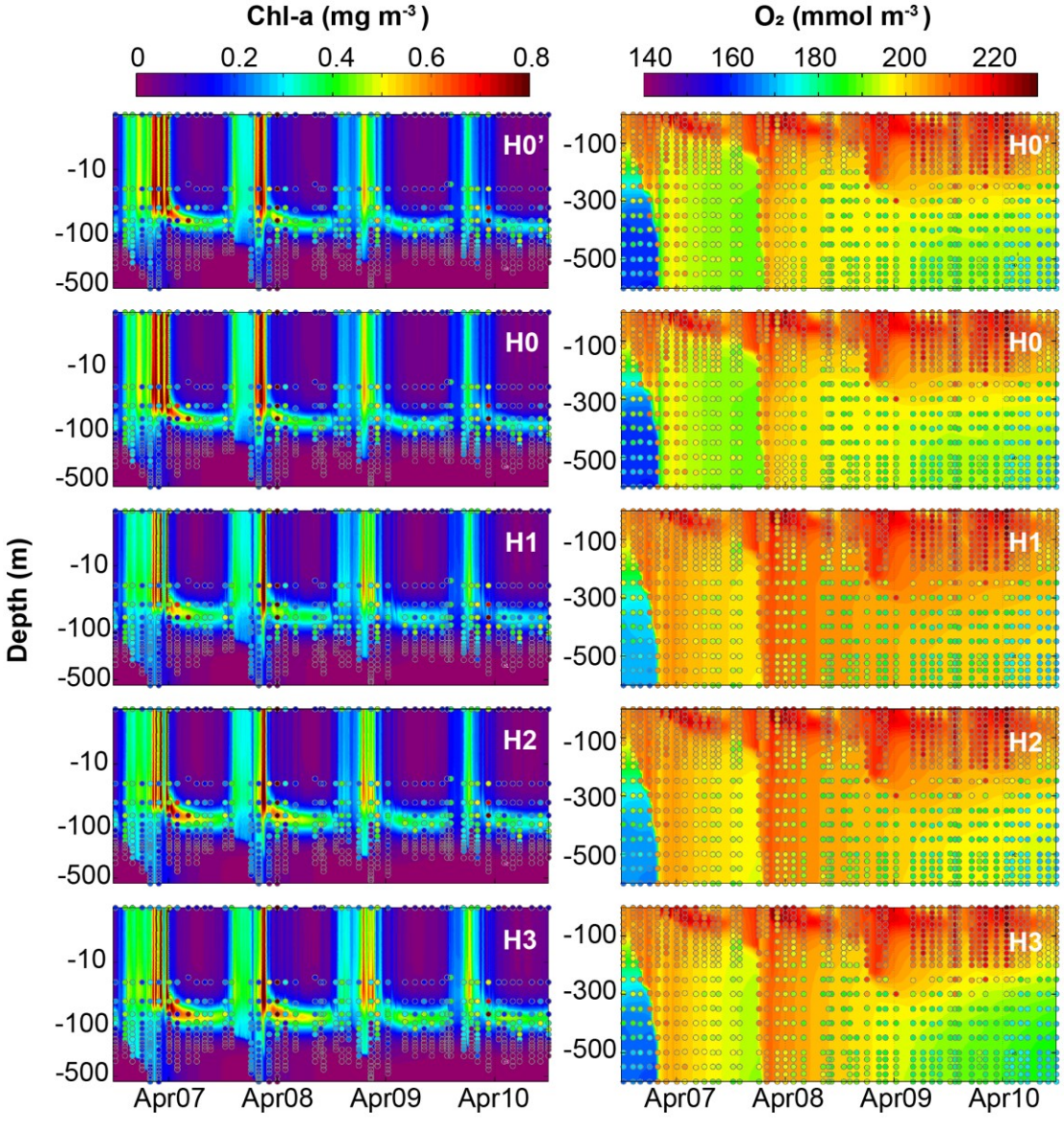

Figure 7: Observed (coloured circles) and simulated (background) Chl-a and O_2 using model versions H0' (no sediment denitrification – no fixers), H0 (no nitrogen fixers), H1 (generic autotrophic fixer), H2 (unicellular and colonial autotrophic fixers), H3 (heterotrophic, and unicellular and colonial autotrophic fixers). Vertical scale in the Chl-a subplots is logarithmic to exaggerate the surface. The spin-up period is not shown.

Biogeosciences Discuss., https://doi.org/10.5194/bg-2017-550
Manuscript under review for journal Biogeosciences
Discussion started: 19 January 2018

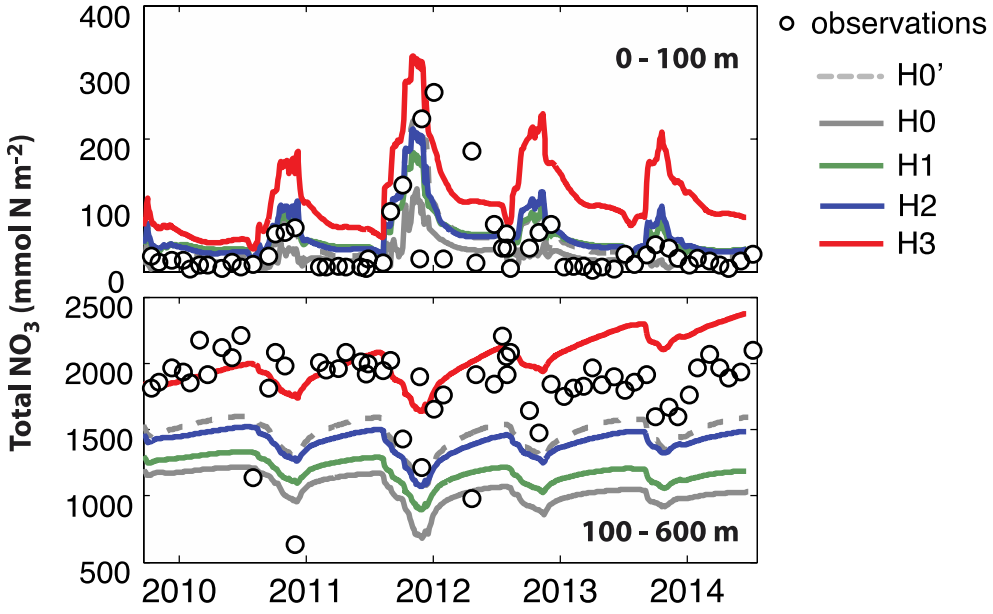

Figure 8: Observed (circles) and simulated (lines) total nitrate in the surface and deep waters at Station A during the model validation period from 2010 to 2014.

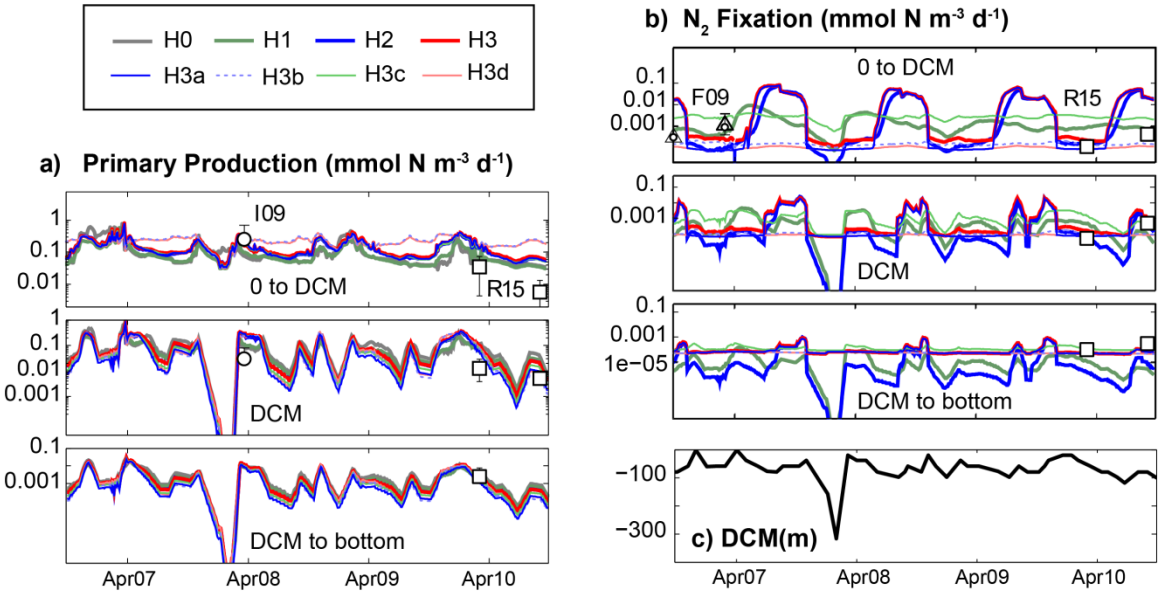

Figure 9: Comparison of previously reported in situ measurements and model results of primary production (a) and N_2 fixation rates (b), averaged at three depth levels. Depth levels are from the surface to the Deep Chlorophyll Maximum, at the DCM and below it. (c) DCM estimated from observed Chl-a profiles at Station A. I09, F09 and R15 refer to Iluz et al., (2009), Foster et al., (2009), and Rahav et al., (2015), respectively .

Biogeosciences Discuss., https://doi.org/10.5194/bg-2017-550
Manuscript under review for journal Biogeosciences
Discussion started: 19 January 2018

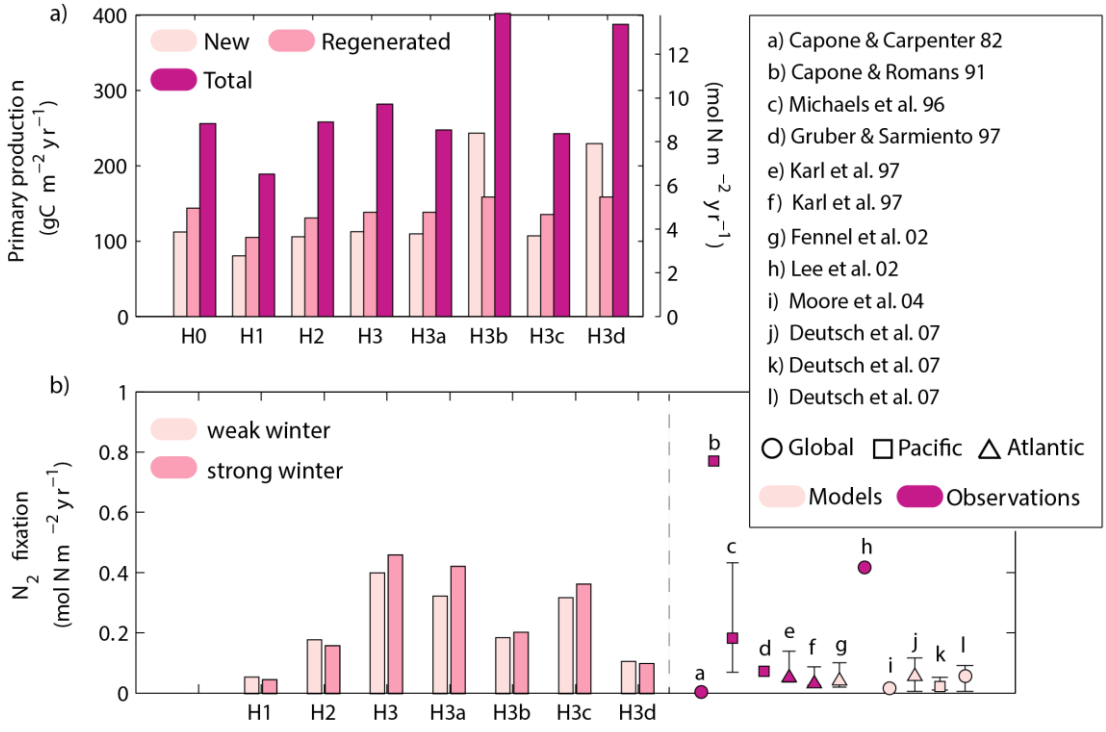

Figure 10: Simulated new, regenerated, and total primary production (a) and N_2 fixation rates (b) obtained by the different simulations (see Table 1for key to different simulations). A summary of previous estimates of N_2 fixation rates in observational and model studies is included in (b). Redfield C:N ratio is used to transform the model results nitrogen units to carbon units.

Table 1: Summary of model version characteristics and assumptions about diazotroph groups. N = no diazotrophs; A = autotrophic diazotrophs; H = heterotrophic diazotrophs. Checkmarks (✓) represent presence of a model characteristic / functional diazotrophic group in the model; dashes represent their absence.

Model Version	Characteristics / Diazotrophs Groups	Denitrification	Generic (A)	Unicellular (A)	Colonial (A)	Heterotrophic (H)
H0	N	✓	-	-	-	-
H0'	N	-	-	-	-	-
H1	A	✓	✓	-	-	-
H2	A	✓	-	✓	✓	-
H3	A H	✓	-	✓	✓	✓
H3a	A H	✓	-	-	✓	✓
H3b	A H	✓	-	✓	-	✓
H3c	A H	✓	✓	-	-	✓
H3d	H	✓	-	-	-	✓
	Diazotrophs characteristics:					
	Inorganic phosphorus uptake		✓	✓	✓	✓

Organic phosphorus uptake	-	-	-	✓
Light growth limitation	✓	✓	✓	-
Temperature dependent maximum growth rate	✓	✓	✓	✓
Minimum temperature limit for growth (20°C)	-	-	✓	-
Predation	-	✓	-	-

Table 2: Parameters used in the base biogeochemical model (H0), including minimum and maximum parameters ranges based on the literature. Parameters values followed by * were obtained by the optimization.

Parameters	Value	Range	Description	Units	References
μ_{Phy}^{0}	0.76*	0.1 – 3	Reference phytoplankton maximum growth rate at T = 0ºC	d^{-1}	a, b, c
$k_{Phy}^{NO_3}$	0.05	0.01 – 0.5	Phytoplankton NO_3 uptake half-saturation	mmol m^{-3}	d, e
$k_{Phy}^{NH_4}$	0.1*	0.01 – 0.5	Phytoplankton NH_4 uptake half-saturation	mmol m^{-3}	d, e
k_{Phy}^{DIP}	0.004*	0.001 – 0.5	Phytoplankton DIP uptake half-saturation	mmol m^{-3}	a, f, g
α_{Phy}	0.1*	0.01 – 0.125	Phytoplankton, initial slope of photosynthetic response	molC $gChl^{-1}$ $(W m^{-2})^{-1}$ d^{-1}	d, h
m_{Phy}	0.1	0.01 – 0.2	Phytoplankton mortality rate	d^{-1}	d
g_{Phy}^{max}	1.16*	0.1 - 4	Zooplankton maximum grazing rate	d^{-1}	b, i
k_{Zoo}^{Phy}	0.5*	0.01 – 0.5	Square zooplankton grazing half-saturation	$(mmol\ m^{-3})^2$	d, e
l_{BM}	0.011*	0.01 – 0.15	Zooplankton base metabolic rate	d^{-1}	d
l_E	0.1	0.05 – 0.35	Zooplankton excretion rate	d^{-1}	d
m_Z	0.35*	0.02 - 0.35	Zooplankton mortality rate	d^{-1}	d
τ	0.1	0.01 - 25	Small detritus aggregation rate	d^{-1}	d, e
θ_{Phy}^{max}	0.142*	0.015 – 0.15	Maximum chlorophyll to carbon ratio	mg Chl $(mg\ C)^{-1}$	h
β	0.74*	0.25 – 0.75	Zooplankton assimilation efficiency	non-dim.	j, k
r_{DOM}	0.2	0.05 – 0.5	DOM remineralization rate	d^{-1}	l
r_D	0.01	0.005 – 0.15	Detritus remineralization rate	d^{-1}	l, m
n_{max}	0.3*	0.01 – 0.35	Nitrification rate	d^{-1}	d, e
k_I	0.1	0.01 – 0.5	Half-saturation radiation for	Wm^{-2}	d

			nitrification inhibition		
I_{th}	0.0095	0.005 – 0.01	Radiation threshold for nitrification inhibition	Wm^{-2}	d
w_{Phy}	0.1	0.01 – 1	Vertical sinking velocity for non-fixing phytoplankton	md^{-1}	n
w_{DL}	-4.44*	0.01 – 25	Vertical sinking velocity for large detritus	md^{-1}	d

a. Fennel et al. (2002) b. Fahnenstiel et al. (1995) c. Veldhuis et al. (2005) d. Fennel et al. (2006) e. (Lima and Doney (2004) f. Ward et al. (2013) g. Moore, et al.(2002) h. Geider et al. (1997) i. Gifford et al. (1995) j. Landry et al. (1984) k. Tande and Slagstad (1985) l. Amon and Benner (1996) m. Enríquez et al. (1993) n. Smayda and Bienfang (1983)

Table 3: Diazotrophs parameters and re-calibrated non-fixing phytoplankton parameters for each model version. H0 = no N2 fixers; H1 = generic autotrophic diazotrophs; H2 = unicellular and colonial cyanobacteria; H3 = heterotrophs, unicellular and colonial cyanobacteria.

Model version:	H0	H1	H2	H3	Units	Description
μ_{Phy}^{0}	0.76	2.20	1.5	1.5	d^{-1}	Reference phytoplankton maximum growth rate at T = 0ºC
θ_{Phy}^{max}	0.022	0.076	0.076	0.05	mg Chl (mg C)$^{-1}$	Maximum chlorophyll to carbon ratio – non fixing phytoplankton
$k_{Phy}^{NH_4}$	0.076	0.076	0.076	0.076	mmol m^{-3}	Phytoplankton NH_4 uptake half-saturation
k_{Phy}^{DIP}	0.001	0.015	0.015	0.015	mmol m^{-3}	Phytoplankton DIP uptake half-saturation
m_{Phy}	0.1	0.06	0.06	0.06	d^{-1}	Phytoplankton mortality rate
g_{Phy}^{max}	1.16	4.0	1.95	1.95	d^{-1}	Zooplankton maximum grazing rate
β	0.36	0.7	0.7	0.7	non-dim.	Zooplankton assimilation efficiency
$\mu_{G_F}^{0}$	-	0.25	-	-	d^{-1}	Reference generic diazotrophs maximum growth rate at T = 0ºC
$k_{G_F}^{DIP}$	-	0.001	-	-	mmol m^{-3}	Generic diazotrophs DIP uptake half-saturation
θ_{F}^{max}	-	0.053	-	-	mg Chl (mg C)$^{-1}$	Maximum chlorophyll to carbon ratio – generic diazotrophs
α_{G_F}	-	0.01	-	-	molC $gChl^{-1}$ $(W m^{-2})^{-1}$ d^{-1}	Generic diazotrophs, initial slope of photosynthetic response
m_{G_F}	-	0.18	-	-	d^{-1}	Generic diazotrophs mortality rate
l_{G_F}	-	0.05	-	-	d^{-1}	Generic diazotrophs respiration rate
$\mu_{U_F}^{0}$	-	-	0.25	0.25	d^{-1}	Reference unicellular cyanobacteria maximum growth rate at T = 0ºC

Biogeosciences Discuss., https://doi.org/10.5194/bg-2017-550
Manuscript under review for journal Biogeosciences
Discussion started: 19 January 2018

Model version:	H0	H1	H2	H3	Units	Description
$k_{U_F}^{DIP}$	-	-	0.004	0.004	mmol m^{-3}	Unicellular cyanobacteria DIP uptake half-saturation
$\theta_{U_F}^{max}$	-	-	0.053	0.053	mg Chl (mg C)$^{-1}$	Maximum chlorophyll to carbon ratio – unicellular cyanobacteria
α_{U_F}	-	-	0.05	0.05	molC gChl^{-1} (W m^{-2})$^{-1}$ d^{-1}	Unicellular cyanobacteria, initial slope of photosynthetic response
m_{U_F}	-	-	0.20	0.2	d^{-1}	Unicellular cyanobacteria mortality rate
l_{U_F}	-	-	0.05	0.05	d^{-1}	Unicellular cyanobacteria respiration rate
$g_{U_F}^{max}$	-	-	0.2	0.2	d^{-1}	Zooplankton maximum grazing rate on unicellular cyanobacteria
$k_{Zoo}^{U_F}$	-	-	0.001	0.001	(mmol m^{-3})^2	Square zooplankton grazing half-saturation on unicellular cyanobacteria
$\mu_{C_F}^0$	-	-	0.25	0.25	d^{-1}	Reference colonial cyanobacteria maximum growth rate at T = 0ºC
$k_{C_F}^{DIP}$	-	-	0.004	0.004	mmol m^{-3}	Colonial cyanobacteria DIP uptake half-saturation
$\theta_{C_F}^{max}$	-	-	0.053	0.053	mg Chl (mg C)$^{-1}$	Maximum chlorophyll to carbon ratio – colonial cyanobacteria
α_{C_F}	-	-	0.05	0.05	molC gChl^{-1} (W m^{-2})$^{-1}$ d^{-1}	Colonial cyanobacteria, initial slope of photosynthetic response
m_{C_F}	-	-	0.18	0.05	d^{-1}	Colonial cyanobacteria mortality rate
l_{C_F}	-	-	0.05	0.18	d^{-1}	Colonial cyanobacteria respiration rate
$\mu_{H_F}^0$	-	-	-	0.2	d^{-1}	Reference heterotrophs maximum growth rate at T = 0ºC
$k_{H_F}^{DIP}$	-	-	-	0.001	mmol m^{-3}	Heterotrophs DIP uptake half-saturation
$k_{H_F}^{DS}$	-	-	-	0.001	mmol m^{-3}	Heterotrophs organic phosphorus uptake half-saturation
m_{H_F}	-	-	-	0.2	d^{-1}	Heterotrophs mortality rate
l_{H_F}	-	-	-	0.05	d^{-1}	Heterotrophs respiration rate

Biogeosciences Discuss., https://doi.org/10.5194/bg-2017-550
Manuscript under review for journal Biogeosciences
Discussion started: 19 January 2018

Table 4 Root-mean-square-errors between observations and corresponding simulated variables. Observations between 2005 and 2010 were used during model calibrations (i.e., assimilated). Observations between 2011 and 2014 are used for independent model validations (non-assimilated)

0-100 m								
	2005 – 2010 (assimilated)				**2011 – 2014 (non-assimilated)**			
	NO_3	**PO_4**	**CHL**	**O_2**	**NO_3**	**PO_4**	**CHL**	**O_2**
H0	0.71	0.04	0.15	7.57	0.60	0.04	0.16	6.39
H1	0.77	0.04	0.14	6.99	0.66	0.04	0.15	7.08
H2	0.78	0.04	0.14	6.96	0.75	0.04	0.14	6.66
H3	1.04	0.05	0.14	7.35	1.50	0.05	0.13	6.22
H3a	1.04	0.06	0.12	7.10	1.41	0.09	0.14	6.47
H3b	1.91	0.05	0.14	7.94	2.15	0.05	0.16	8.13
H3c	1.01	0.06	0.12	7.05	1.06	0.08	0.14	6.55
H3d	1.60	0.05	0.19	7.91	1.78	0.05	0.19	8.21
100 – 600 m								
	NO_3	**PO_4**	**CHL**	**O_2**	**NO_3**	**PO_4**	**CHL**	**O_2**
H0	1.53	0.05	0.08	15.54	2.26	0.06	0.06	17.34
H1	1.43	0.05	0.07	15.09	2.02	0.05	0.06	21.70
H2	1.29	0.05	0.07	14.17	1.56	0.04	0.06	17.57
H3	1.05	0.05	0.07	13.28	0.89	0.05	0.06	10.03
H3a	1.12	0.05	0.07	13.42	0.93	0.07	0.06	11.98
H3b	1.26	0.10	0.07	18.29	1.51	0.14	0.06	29.99
H3c	1.14	0.05	0.07	14.37	1.18	0.05	0.06	16.16
H3d	1.41	0.11	0.14	18.39	1.85	0.14	0.13	30.38